Lixin Cheng
Laboratory of Heat and Mass Transfer (LTCM),
Faculty of Engineering (STI),
École Polytechnique Fédérale de Lausanne
(EPFL),
Station 9,
Lausanne CH-1015, Switzerland
e-mail: lixincheng@hotmail.com

Gherhardt Ribatski
Department of Mechanical Engineering,
Escola de Engenharia de São Carlos (EESC),
University of São Paulo (USP),
São Carlos, São Paulo 13566-590, Brazil
e-mail: ribatski@sc.usp.br

John R. Thome
Laboratory of Heat and Mass Transfer (LTCM),
Faculty of Engineering (STI),
École Polytechnique Fédérale de Lausanne
(EPFL),
Station 9,
Lausanne CH-1015, Switzerland
e-mail: john.thome@epfl.ch

Two-Phase Flow Patterns and Flow-Pattern Maps: Fundamentals and Applications

A comprehensive review of the studies of gas-liquid two-phase flow patterns and flow-pattern maps at adiabatic and diabatic conditions is presented in this paper. Especially, besides other situations, this review addresses the studies on microscale channels, which are of great interest in recent years. First, a fundamental knowledge of two-phase flow patterns and their application background is briefly introduced. The features of two-phase flow patterns and flow-pattern maps at adiabatic and diabatic conditions are reviewed, including recent studies for ammonia, new refrigerants, and CO_2. Then, fundamental studies of gas-liquid flow patterns and flow-pattern maps are presented. In the experimental context, studies of flow patterns and flow-pattern maps in macro- and microscale channels, across tube bundles, at diabatic and adiabatic conditions, under microgravity and in complex channels are summarized. In addition, studies on highly viscous Newtonian fluids (non-Newtonian fluids are beyond the scope of this review) are also mentioned. In the theoretical context, modeling of flow-regime transitions, specific flow patterns, stability, and interfacial shear is reviewed. Next, flow-pattern-based heat transfer and pressure drop models and heat transfer models for specific flow patterns such as slug flow and annular flow are reviewed. Based on this review, recommendations for future research directions have been given. [DOI: 10.1115/1.2955990]

1 Introduction

Gas-liquid two-phase flows at both adiabatic and diabatic conditions are very complex physical processes since they combine the characteristics of deformable interface, channel shape, flow direction, and, in some cases, the compressibility of one of the phases. In addition to inertia, viscous and pressure forces present in a single-phase flow and two-phase flows are also affected by the interfacial tension forces, the wetting characteristics of the liquid on the tube wall (contact angle), and the exchange of mass, momentum, and energy between the liquid and vapor phases. Depending on the operating conditions, such as pressure, temperature, mass velocity, adiabatic or diabatic flow, channel orientation (the effect of gravity, which in nonvertical channels tends to pull the liquid to the bottom of the channel), and fluid properties (widely different combinations of different classes of fluids such as air-water, steam-water and liquid and vapor phases of refrigerants), various gas-liquid interfacial geometric configurations occur in two-phase flow systems. These are commonly referred to as flow patterns or flow regimes. Many different flow patterns have been defined by various researchers [1–4], and the nature of the flow patterns varies with channel geometry and size (macro- and microscale), fluid physical properties, flow orientation, flow parameters, adiabatic or diabatic condition, etc. Furthermore, transient two-phase flows and flow oscillations are also important topics but are beyond the scope of the present review.

Both flow patterns at adiabatic and diabatic conditions are important in the study of two-phase flows. Generally, the gas and liquid flow rates are constant for adiabatic flows, although in high speed flow (as in critical flow) partial vaporization of the liquid may occur even though there is no heat addition. Gas dissolution or desorption in the liquid phase may also contribute in some instances to mass exchange in gas-liquid flows, especially for fluoroinerts. One example of adiabatic two-phase flows is the transportation of gas-oil mixtures in pipelines. Diabatic two-phase flows with heat transfer occur during flow boiling, flow condensation, or gas-liquid two-phase flows with heat addition or removal. These are confronted in steam generators, boiling water reactors, boiling and condensation of refrigerants used in air conditioning, refrigeration and heat pump systems, petrochemical processes, and so on. Without knowing the local flow patterns, one cannot correctly calculate the thermal/hydraulic design parameters. In fact, the physical mechanisms controlling two-phase pressure drops and heat transfer coefficients are intrinsically related to the local flow patterns [1–4], [10–23], and thus flow-pattern prediction is an important aspect of two-phase heat transfer and pressure drops.

To predict local flow patterns, two-phase flow-pattern maps are used. These are generally two-dimensional graphs with transition criteria to separate the areas corresponding to the various flow regimes. Over the past decades, numerous studies of flow patterns have been conducted for various tube configurations such as inside vertical, horizontal, and inclined channels (macro- and microchannels) and other complex geometries such as inside enhanced tubes, in compact heat exchangers, across tube bundles, and under microgravity conditions, for which numerous flow-pattern maps have been proposed. Most flow-pattern maps have been developed for adiabatic conditions, e.g., the Hewitt and Roberts [5] flow-pattern map for vertical upflow and the Baker [6], Taitel and Dukler [7], Hashitume [8], and Steiner [9] flow maps for horizontal flow, just to name a few. Regarding diabatic flow-pattern maps, they should include the effect of heat flux and dryout on the flow-pattern transition boundaries and revert to an adiabatic map when the heat flux tends to zero. In principle, adiabatic two-phase flow maps are not applicable to diabatic conditions, although this is often done. Such extrapolation of adiabatic flow maps to diabatic conditions is, in general, not reliable and also lacks the influence of heat transfer on the local flow patterns and their transitions. With respect to diabatic two-phase flows, one of the earliest diabatic flow-pattern maps is that of Kattan–Thome–Favrat [10–12], which was developed according to their experimental observations and heat transfer data for five refrigerants (R-134a, R123, R402a, R404a, and R502) under evaporation conditions. Their flow map was then the basis of their flow boiling heat transfer model for evaporation in horizontal tubes in the fully stratified,

Published online July 30, 2008. Transmitted by Assoc. Editor J. N. Reddy.

stratified-wavy, intermittent, and annular flow regimes and for annular flow with partial dryout at the top of the tube. Physically, it is connected to the local heat transfer characteristics and mechanisms by use of simplified two-phase flow structures to account for any dry perimeter predicted to occur and may be applied to both adiabatic and diabatic conditions. Since then, a number of modified flow maps have been developed for different fluids such as R134a, R407c, R22, R410A, ammonia (R717), and CO_2 (R747) under evaporation and/or condensation conditions [13–23] on the basis of the Kattan–Thome–Favrat flow map. These will be discussed in Secs. 2–4.

The vast majority of technical calculations on two-phase flows are made without any reference whatsoever to flow patterns. Nearly all two-phase pressure drop correlations in the literature and reference books are purely empirical without reference to the flow patterns that they cover. These include such leading methods as those of Martinelli and Nelson [24], Lockhart and Martinelli [25], Chisholm [26], Grönnerud [27], Müller-Steinhagen and Heck [28], and Friedel [29]. Furthermore, most of the leading flow boiling heat transfer correlations do not contain any information on the flow patterns, such as those of Chen [30], Shah [31], Gungor and Winterton [32], and Kandlikar [33]. Such methods are typically most accurate for annular flow, but in fact they cannot themselves identify when this regime occurs, nor do they use explicitly an annular flow structure in the prediction method.

This poses the following question: Are flow patterns and flow-pattern maps helpful in practical design? Certainly, this seems to be the case. The relationships for two-phase pressure drops are likely to be significantly different for a flow consisting of a dispersion of bubbles (bubbly flow) than for a flow consisting of a liquid film on the channel wall with a central gas core (annular flow). Recent work has demonstrated that two-phase pressure drops can be more accurately predicted by giving attention to specific flow patterns in a general flow-pattern-based model [22,34–36]. Furthermore, models that have a sound theoretical basis are more likely to be reliable and generally applicable than those that are purely empirical. Calculation methods based on flow patterns and flow-pattern maps accounting for two-phase flow structure effects will ultimately supersede those ignoring the influence of the flow regimes. For heat transfer, the aforementioned flow-pattern-based heat transfer models [10–23] provide more accurate heat transfer predictions and attempt to intrinsically relate the heat transfer mechanisms to the local flow patterns. Therefore, flow patterns and flow-pattern maps play an important role in improving the prediction models for two-phase pressure drops and heat transfer coefficients.

The earliest papers on flow patterns and flow-pattern maps date back to the early 1950s, and after that an avalanche of papers have been published on this subject. Numerous research reviews on flow patterns have been presented by different authors. Rouhani and Sohal [37] presented an overall literature review covering commonly observed flow regimes in horizontal and vertical pipes, different types of flow pattern maps, experimental techniques for direct and indirect determination of flow regimes, flow-regime transition criteria based on correlations and theoretical derivations, and also the effects of wall roughness, heat flux, and flow accelerations on flow-regime transitions. Collier and Thome [1], Carey [2], Hewitt [3], and Thome [4] also provided summaries or reviews on two-phase flow patterns and flow maps. Generally, they provided an introduction to the fundamental knowledge for conventional size channels with various orientations, such as horizontal, vertical, and inclined channels. However, they did not provide information on two-phase flow patterns and flow maps in microscale channels. Therefore, this review also addresses the studies on microscale channels.

In recent years, emphasis has been put on the characteristics of two-phase flow and heat transfer in small and microscale flow passages due to the rapid development of microscale devices [38–48]. Due to the significant differences of transport phenomena in microscale channels as compared to conventional size channels or macroscale channels, one very important issue should be clarified about the distinction between microscale and macroscale channels. However, a universal agreement is not clearly established in the literature. Instead, there are various definitions on this issue.

Shah [45] defined a compact heat exchanger as an exchanger with a surface area density ratio $>700\ m^2/m^3$. This limit translates into a hydraulic diameter of <6 mm. According to this definition, the distinction between macro- and microscale channels is 6 mm.

Mehendale et al. [46] defined various small and mini heat exchangers in terms of hydraulic diameter D_h:

- micro heat exchanger: $D_h = 1-100\ \mu m$
- meso heat exchanger: $D_h = 100\ \mu m - 1$ mm
- compact heat exchanger: $D_h = 1-6$ mm
- conventional heat exchanger: $D_h > 6$ mm

According to this definition, the distinction between macro- and microscale channels is somewhere between 1 mm and 6 mm.

Based on engineering practice and application areas such as refrigeration industry in the small tonnage units, compact evaporators employed in automotive, aerospace, air separation, and cryogenic industries, cooling elements in the field of microelectronics, and microelectromechanical systems (MEMS), Kandlikar [38] defined the following ranges of hydraulic diameters D_h, which are attributed to different channels:

- conventional channels: $D_h > 3$ mm
- minichannels: $D_h = 200\ \mu m - 3$ mm
- microchannels: $D_h = 10-200\ \mu m$

According to this definition, the distinction between small and conventional size channels is 3 mm.

There are several important dimensionless numbers, which are used to represent the feature of fluid flow in microscale channels. According to these dimensionless numbers, the distinction between macro- and microscale channels may be classified as well. Triplett et al. [47] defined flow channels with hydraulic diameters D_h of the order of, or smaller than, the Laplace constant L,

$$L = \sqrt{\frac{\sigma}{g(\rho_L - \rho_G)}} \tag{1}$$

as microscale channels, where σ is the surface tension, g is the gravitational acceleration, and ρ_L and ρ_G are, respectively, liquid and gas/vapor densities.

Kew and Cornwell [43] earlier proposed the confinement number Co for the distinction of macro- and microscale channels,

$$\mathrm{Co} = \frac{1}{D_h}\sqrt{\frac{4\sigma}{g(\rho_L - \rho_G)}} \tag{2}$$

which is actually based on the definition of the Laplace constant.

Based on a linear stability analysis of stratified flow and the argument that neutral stability should consider a disturbance wavelength of the order of channel diameter, Brauner and Moalem-Maron [48] derived the Eotvös number Eö criterion for the dominance of surface tension for microscale channels,

$$\mathrm{E\ddot{o}} = \frac{(2\pi)^2\sigma}{(\rho_L - \rho_G)D_h^{\,2}g} > 1 \tag{3}$$

The definition of a microscale channel is quite confusing because there are different criteria available as described above. Cheng and Mewes [42] made a comparison of these different criteria for microscale channels. Figure 1 shows their comparable results for water and CO_2, which shows the big difference among these criteria. So far, the distinction of microscale channels is still in dispute. In this review, the distinction between macro- and mi-

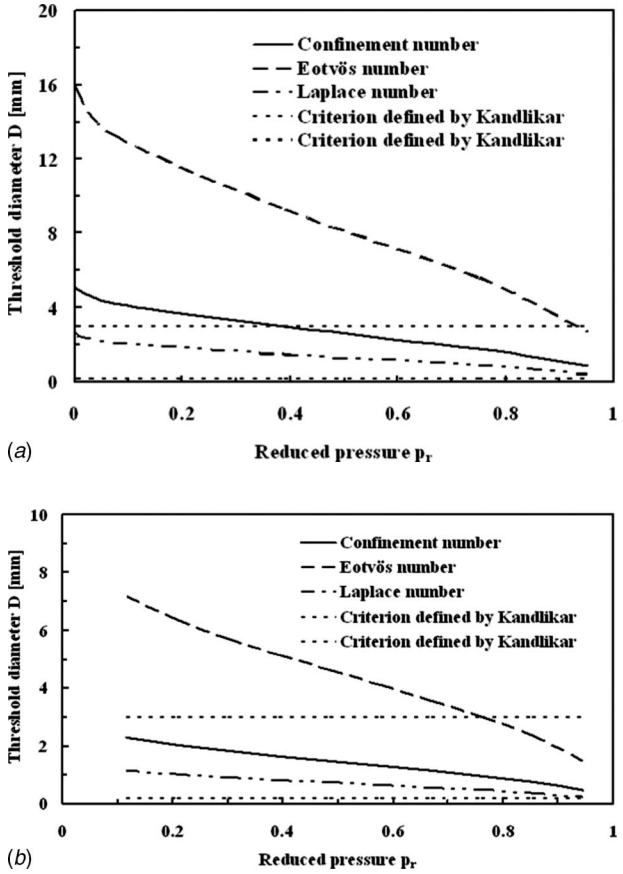

Fig. 1 Comparison of various definitions of threshold diameters for microscale channels: (*a*) water and (*b*) CO_2 by Cheng and Mewes [42]

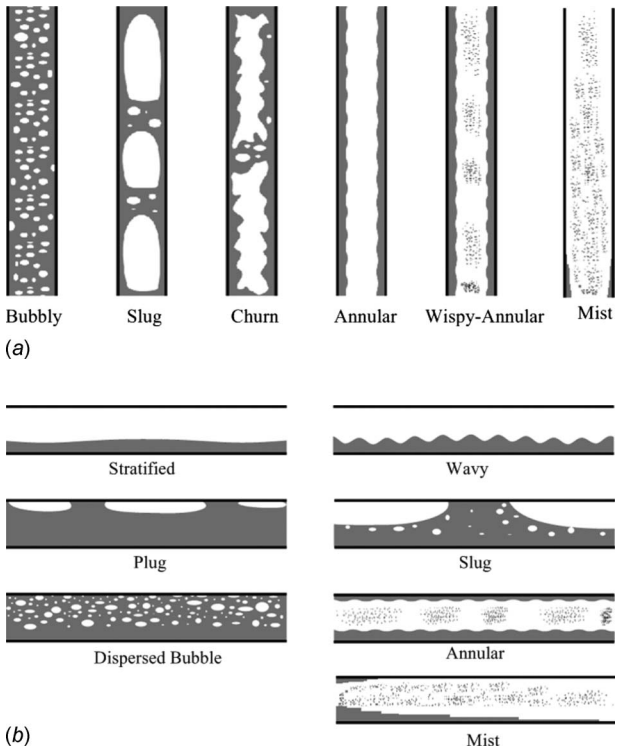

Fig. 2 (*a*) Schematic of flow patterns in vertical upward gas-liquid cocurrent flow; (*b*) schematic of flow patterns in horizontal gas-liquid cocurrent flow [1]

croscale channels by the threshold diameter of 3 mm is adopted due to the lack of a well-established theory but is in line with those recommended by Kandlikar [38]. Using this threshold diameter enables more relevant studies to be included.

So far, there is a little information on two-phase flow patterns at microgravity conditions and in complex configurations such as tube bundles, enhanced channels, U-bends, heat exchangers, and so on. In addition, only a limited number of studies have been done on two-phase flow patterns during condensation. Furthermore, a number of theoretical studies have been performed on specific flow patterns and flow-pattern instabilities. Therefore, the present paper aims to address many of these related topics and to provide a comprehensive review of what has been learned from this research. It should be mentioned that only Newtonian and highly viscous Newtonian fluids are addressed here (non-Newtonian fluids are beyond the scope of this review).

In what follows, different aspects of flow patterns in a general scope are first presented, and published literatures are mentioned in accordance to their relevance to the specific topics. Then, several leading flow-pattern maps will be presented together with a discussion of their limitations and future requirements. Following this, a detailed review of the studies classified according to specific topics will be presented. Finally, attention will be turned to flow-pattern-based heat transfer and pressure drop models.

2 Schematics of Two-Phase Flow Patterns and Flow-Pattern Maps

First, because of the variety of names and definitions of flow patterns, a discussion of flow patterns in vertical and horizontal tubes for adiabatic and diabatic conditions is presented. Then, several leading flow-pattern maps are presented and their limitations are discussed.

2.1 Flow Patterns. In this section, flow patterns for adiabatic and diabatic conditions are described and discussed by category.

Vertical Adiabatic Two-Phase Flows. Figure 2(*a*) shows the most commonly observed two-phase flow patterns in a vertical tube. Bubbly flow occurs when a relatively small quantity of gas or vapor is mixed with a moderate flow rate of liquid. Increasing the gas flow rate may lead to plug flow, which some observers call the Taylor bubble flow. With further increase in gas flow rate, one may observe slug flow, which consists of a regular train of large bubbles separated by liquid slugs. Each of these bubbles occupies nearly the entire channel cross section except for a thin liquid layer on the wall, and their length is typically one to two times the channel diameter. An increase in both gas and liquid flow rates will lead to an unstable flow pattern, which is called churn flow. A relatively higher gas flow rate generates a wispy-annular flow pattern, which is not observed or recognized as such in many studies. Very high gas flow rates may cause some of the liquid flow to be entrained as droplets carried along with the continuous gas phase in annular flows. At even higher gas flow rates, all the liquid is sheared from the wall to form the mist flow regime.

Horizontal Adiabatic Two-Phase Flows. Figure 2(*b*) shows the most commonly observed flow patterns for cocurrent flow of gas and liquid in a horizontal tube. Two-phase flow patterns in a horizontal tube are similar to those in a vertical tube, but distribution of the liquid is influenced by gravity. In general, most flow patterns in horizontal tubes show a nonsymmetrical structure, which is due to the effect of gravity on the different densities of the phases. This generates a tendency toward stratification in the vertical direction, with the liquid having a tendency to occupy the lower part of the channel and the gas, the upper part. Stratified flow is usually observed at relatively low flow rates of gas and

liquid. As the gas and liquid flow rates are increased, the smooth interface of the liquid becomes rippled and wavy. This pattern is called a stratified-wavy flow. If the liquid flow rate is further increased while the vapor flow is maintained low, an intermittent flow pattern will develop in which gas pockets or plugs are entrapped in the main liquid flow and then a plug flow will develop. If flow rates of gas and liquid increase together, a so called slug flow regime will develop. The main distinction between slug and plug flow is in the more pronounced nature of intermittent liquid mass separated by a larger gas bubble. With further increase in the gas flow alone, annular flow will develop. The gas flow in the core of an annular flow may entrain a portion of the liquid phase in the form of droplets, and in some cases the liquid film may also entrain some small bubbles. At relatively large liquid flow rates, with little gas flow, one would observe the so called dispersed bubble flow in which the liquid phase is in the dispersed form of the scattered bubbles. At very high gas flow rates, the mist flow is reached, which can begin at the top perimeter where the annular film is the thinnest and then progress downstream to the bottom perimeter.

Flow Patterns in Inclined Channels. There are relatively few experimental observations on flow patterns in inclined tubes, notwithstanding the technical importance of such flows. Hewitt [3] summarized this topic briefly. In short, flow patterns in inclined channels seem to have the same basic structures as in vertical and horizontal flows except for the limitation or total suppression of the churn regime.

Flow Patterns in Other Applications. A limited amount of information is available in the literature in a variety of other specific applications, which are necessarily mentioned here, such as vertical downward flow and tube bundles. Collier and Thome [1] presented a brief introduction for rectangular channels, internal grooves, helical inserts, obstructions, expansions, contractions, bends, coils, and annuli. Rounhani and Sohal [37] presented a brief summary of downward cocurrent flow. Relatively few studies on flow patterns in cocurrent downward flow are reported in the literature. However, all of the flow patterns of cocurrent upward flow may also appear in the downward flow situations. Hewitt [3] presented a brief summary of flow patterns in complex geometries such as in rod bundles and inside shell and tube heat exchangers. Thome [4] provided some detailed information on flow patterns and flow maps for two-phase flows over horizontal tube bundles. However, there is a scarcity of information on these topics.

Flow Patterns in Countercurrent Flows. There is very little published information regarding flow patterns in countercurrent flow situations. Rounhani and Sohal [37] also presented a brief summary of countercurrent flows. In general, flow regimes in countercurrent flows have a very limited range of existence due to the fact that a continuous increase in the flow rate of either phase would lead to so called flooding, which means that the passage of the other phase would be blocked and cocurrent flow would be established. In horizontal channels, countercurrent flow may exist only as a stratified-smooth or stratified-wavy flow. In vertical channels, it exists only for downward liquid flow against rising vapor. The observed patterns are limited to annular, churn, and plug flows. So far, there is a scarcity of information on this topic.

Flow Patterns at Diabatic Conditions. At diabatic conditions, two-phase heat transfer coefficients and pressure drops are closely related to the local flow patterns and vice versa. Therefore, flow patterns are very important in the heat transfer and pressure drop predictions.

For flow boiling (evaporation), consider a vertical tube heated uniformly over its length with a low heat flux and fed with subcooled liquid at its base at such a rate that the liquid is totally evaporated over the length of the tube. Figure 3 shows the flow patterns in diagrammatic form, the various flow patterns that may

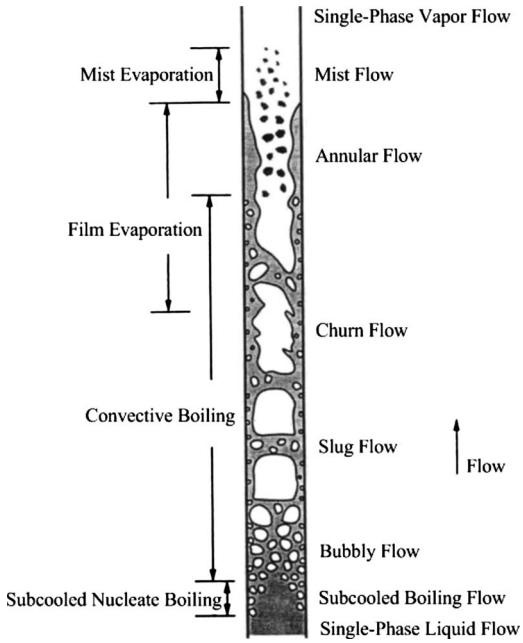

Fig. 3 Schematic of flow patterns and the corresponding heat transfer mechanisms for upward flow boiling in a vertical tube [1,2]

be encountered over the length of a vertical tube heated by a uniform heat flux, together with the corresponding heat transfer regimes. Figure 4 shows a schematic representation of a horizontal tubular channel heated by a uniform heat flux and fed with subcooled liquid. Flow patterns formed during evaporation in a horizontal tube may be influenced by departures from thermodynamic and hydrodynamic equilibrium. Asymmetric phase distributions and stratification introduce additional complications. Important points to note from a heat transfer viewpoint are the possibility of intermittent drying and rewetting of the upper surfaces of the tube in slug and wavy flows and the progressive dryout over long tube lengths of the upper circumference of the tube wall in annular flow. At higher inlet liquid velocities, the influence of gravity is less obvious, the phase distribution becomes more symmetrical, and the flow patterns become closer to those as in vertical flow.

For condensation, Fig. 5 illustrates the flow patterns typically observed during condensation inside a horizontal tube [49]. At the inlet, film condensation around the circumference of the tube pro-

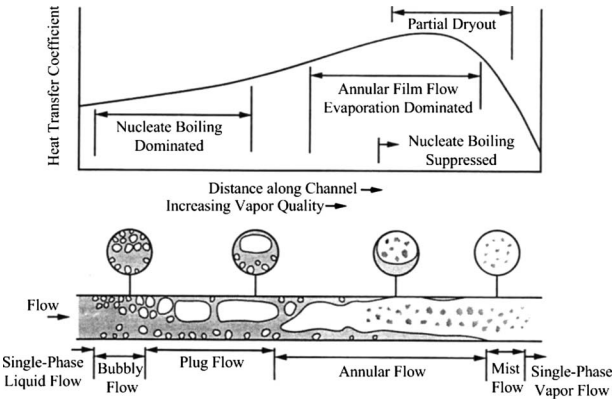

Fig. 4 Schematic of flow patterns and the corresponding heat transfer mechanisms and qualitative variation of the heat transfer coefficients for flow boiling in a horizontal tube [1,2]

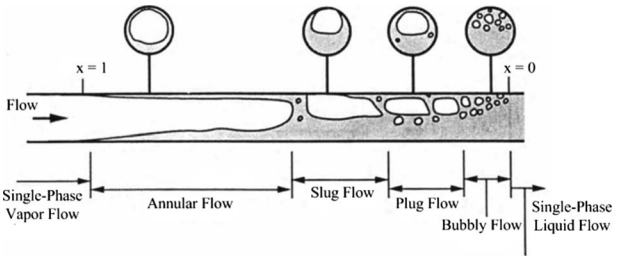

Fig. 5 Schematic of flow patterns for horizontal gas-liquid cocurrent flow in condensation [49]

duces an annular flow, with some droplets entrained in the central high velocity vapor core. As condensation continues, the vapor velocity falls and reduces the influence of vapor shear on the condensate, and the influence of gravity forces increases. At high flow rates, slug and bubble flows are eventually reached, while at low flow rates large magnitude waves and then stratified flow are formed.

2.2 Flow-Pattern Maps. Flow-pattern maps may be classified primarily into two types: empirical flow-pattern maps, which are generally fitted to the observed flow-pattern database and theoretical or semitheoretical flow-pattern maps whose transitions are predicted from physical models of the flow phenomena. Theoretical or semitheoretical flow-pattern maps are developed according to the flow structure and are sometimes related to heat transfer mechanisms and diabatic characteristics. Usually, only two flow parameters are used to define a coordinate system on which the boundaries between the different flow patterns are charted, such as the superficial gas and liquid velocities. Transition boundaries are then proposed to distinguish the location of the various flow regimes as in a classical map. Most flow maps are only valid for a specific set of conditions and/or fluids, although efforts are made to propose generalized flow maps. In this section, only several leading flow-pattern maps are presented. Generally, flow-pattern maps for other applications such as microscale channels, enhanced heat transfer tubes, compact heat exchangers, and tube bundles and at microgravity conditions have been proposed by modification of these leading flow maps.

Empirical Flow-Pattern Maps. One of the best known empirical flow-pattern maps for horizontal flow is that of Baker [6] shown in Fig. 6. It was based on observations of cocurrent flow of gaseous and condensate petroleum products in horizontal pipes

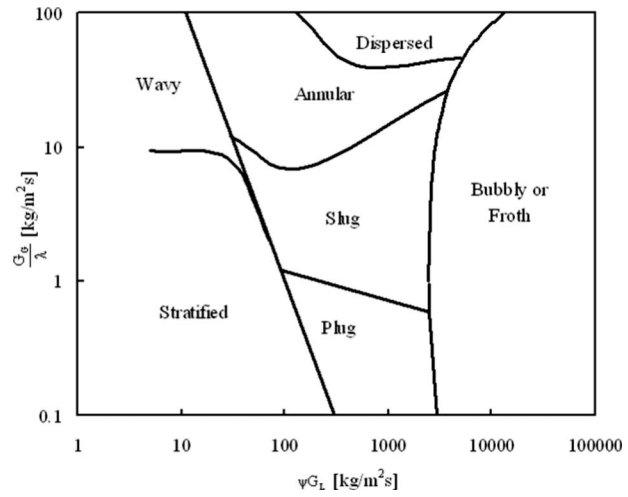

Fig. 6 The Baker [6] flow-pattern map for horizontal gas-liquid cocurrent flow

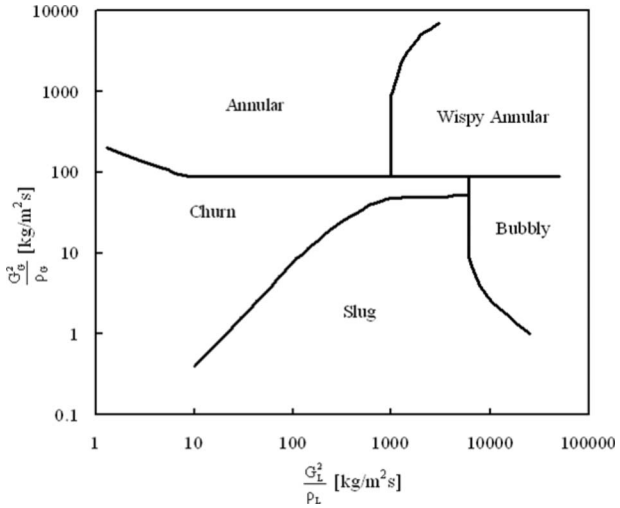

Fig. 7 The Hewitt and Roberts [5] flow-pattern map for vertical upward gas-liquid cocurrent flow

and was constructed with two parameter groups G_G/λ and $G_L\psi$ (where G_G and G_L are gas and liquid mass velocities, respectively), taking into account their physical properties by introducing the following parameters:

$$\lambda = \left(\frac{\rho_G}{\rho_A}\frac{\rho_L}{\rho_W}\right)^{1/2} \tag{4}$$

$$\psi = \left(\frac{\sigma_W}{\sigma}\right)\left[\left(\frac{\mu_L}{\mu_W}\right)\left(\frac{\rho_W}{\rho_L}\right)^2\right]^{1/3} \tag{5}$$

where ρ_A, ρ_W, σ_W, and μ_W are the density of air, the density of water, the surface tension of water, and the dynamic viscosity of water, respectively, at 1 atm pressure and room temperature while ρ_L, ρ_G, σ, and μ_L are the liquid density, gas density, surface tension, and liquid viscosity, respectively. The correction factors λ and ψ had previously been used for correlating data on flooding points in distillation columns. Although Baker's flow map coordinates include these apparently relevant variables for scaling a variety of different conditions, later investigations have shown that this map does not adequately predict horizontal flow regimes in numerous situations, as pointed out by Rounhani and Sohal [37].

One of the leading empirical flow-pattern maps for vertical upflows is that of Hewitt and Roberts [5] shown in Fig. 7. On this map, the coordinates are the superficial momentum fluxes of the respective phases. Both air-water and steam-water data could be represented in terms of this plot, which thus covers a reasonably wide range of fluid physical properties. All the transitions are assumed to depend on the phase momentum fluxes. Wispy-annular flow is a subcategory of annular flow, which occurs at high mass flux when the entrained drops are said to appear as wisps or elongated droplets.

Generally, the accuracy in determining transition lines on a flow map is in part dependent on the number of experiments carried out and on the adopted coordinate systems as well. There are many other coordinate systems for flow-pattern maps used by different investigators, for example, superficial gas and liquid velocities u_{GS} and u_{LS} (m/s), and mass velocities G (kg/m^2 s) versus vapor qualities x. According to Troniewski and Ulbrich [50], the coordinates used in flow maps may be divided into three groups:

(1) Phase velocities or fluxes: gas and liquid superficial velocities u_{GS} and u_{LS} (m/s) or gas and liquid superficial mass fluxes G_{GS} and G_{LS} (kg/m^2 s) and gas and liquid mass flow rates M_G and M_L (kg/s). Use of these parameters, while

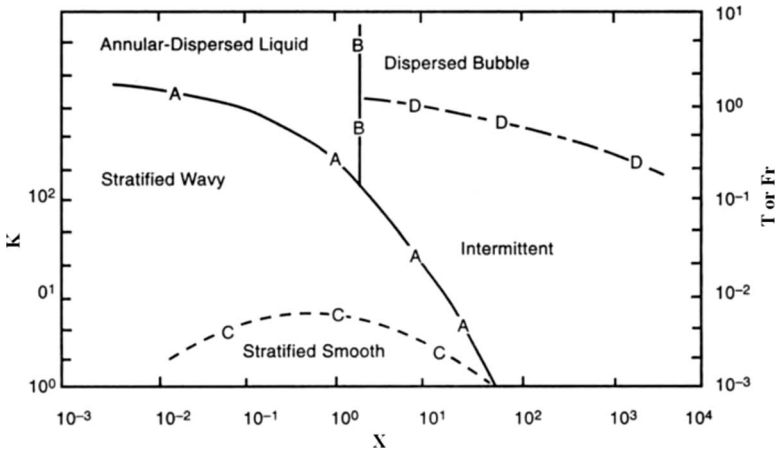

Fig. 8 The Taitel and Dukler [7] flow-pattern map for horizontal gas-liquid cocurrent flow: coordinates of curves *A* and *B* are Fr versus *X*, coordinates of curve *C* are *K* versus *X*, and coordinates of curve *D* are *T* versus *X*

undoubtedly being the most convenient, does not ensure creation of a universal flow-pattern map for different two-phase mixtures.

(2) Quantities referring to the two-phase flow homogeneous model are the transformations of the parameters from group (1) such as total velocity u_T, total mass flux G_T, Froude number based on total velocity Fr_T, void fraction ε, and quality x, and they are only useful for the description of some flow-pattern maps.

(3) Parameters including the physical properties of phases such as liquid and gas Reynolds numbers Re_L and Re_G, Baker correction factors λ and ψ, gas and liquid kinetic energies E_G and E_L, and others; this formulation gives the best possibility for attaining a universal flow-pattern map.

A summary of the coordinates used in flow maps can be found in Refs. [50,51].

Theoretical or Semitheoretical Flow-Pattern Maps. There have been various attempts at a theoretical or semitheoretical description of flow-pattern transitions. For such a description to be successful, it should be suitable for extrapolation to a wide range of conditions. Perhaps the most comprehensive treatment of flow-pattern transitions in horizontal flow on a semitheoretical basis is that of Taitel and Dukler [7]. It has been proven successful in predicting a fairly wide range of system conditions. Figure 8 shows the Taitel and Dukler flow-pattern map. The parameter groups, which are based on semitheoretical derivations for different flow-pattern transitions in horizontal or slightly inclined channels (θ is the angle of inclination), are as follows:

$$X = \left[\frac{(dp/dz)_L}{(dp/dz)_G}\right]^{1/2} \tag{6}$$

$$\mathrm{Fr} = \frac{G_G}{[\rho_G(\rho_L - \rho_G)Dg\cos\theta]^{1/2}} \tag{7}$$

$$T = \left[\frac{|(dp/dz)_L|}{g(\rho_L - \rho_G)\cos\theta}\right]^{1/2} \tag{8}$$

$$K = \mathrm{Fr}\left[\frac{G_L D}{\mu_L}\right]^{1/2} \tag{9}$$

where X is the Martinelli parameter, $(dp/dz)_L$ is the frictional pressure gradient as if the liquid in the two-phase flow were flowing alone in the tube, $(dp/dz)_G$ is the frictional pressure gradient as if the gas in the two-phase flow were flowing alone in the tube, Fr is the Froude number, D is the tube diameter, g is the acceleration due to gravity, ρ_L is the liquid density, ρ_G is the gas density, and μ_L is the liquid viscosity. They suggested the K versus X coordinate with a theoretically derived boundary curve, C, for transition from stratified-smooth to stratified-wavy flow. The Fr versus X relationship was proposed for the transitions between stratified-wavy, annular-dispersed (droplets), dispersed bubble, and intermittent (plug or slug) flows. The theoretically determined transition curves A and B (at $X=1.6$) between the said regimes were also given in those coordinates. Finally, T versus X was proposed for defining the transition between dispersed bubble and intermittent (plug or slug) flow regimes with the transition line D. The transition curves shown in Fig. 8 are for the case of zero inclination angle (horizontal). All the transition criteria used by Taitel and Dukler have some theoretical bases, although they are sometimes rather tenuous. As pointed out by Hewitt [3], it should be remembered that there is an essential arbitrariness in the interpretation of flow-pattern data, and thus it is unlikely that perfect prediction methods will ever emerge.

Diabatic Flow-Pattern Maps. In the case of diabatic two-phase flows such as flow boiling (evaporation) and condensation, very few maps have been proposed. Important factors influencing these flows and their transitions are nucleate boiling, evaporation or condensation of liquid films on what could otherwise be dry parts of the perimeter, and acceleration or deacceleration of the flows. For example, nucleate boiling in an annular film tends to increase the film's thickness and change the void profile near the wall, or vigorous nucleate boiling in an otherwise stratified flow can completely wet the upper perimeter, thus increasing liquid entrainment in the vapor core. It is desirable that diabatic flow-pattern maps include the influences of heat flux, dryout, etc., on the flow-pattern transition boundaries. One such map is that of Kattan–Thome–Favrat [10–12] for evaporation inside horizontal channels. This was developed based on five refrigerants (pure fluids R134a and R123, the azeotropic refrigerant mixture R502, and two near azeotropic mixtures R402A and R404A) under flow boiling conditions by modification of the Steiner map [9], which in turn is a modified Taitel–Dukler flow map [7]. Figure 9 shows the Kattan–Thome–Favrat flow-pattern map (solid lines) [10–12] compared to the Steiner map [9] (dashed lines) evaluated for R410A at $T_{\mathrm{sat}}=5\,^{\circ}\mathrm{C}$ in a 13.84 mm internal diameter tube at different heat fluxes [36]. In the Kattan–Thome–Favrat flow map, stratified, stratified-wavy, intermittent, annular, bubbly, and mist flows are encountered. The map includes a diabatic method for predicting the anticipation of the onset of dryout at the top of the tube in evaporating annular

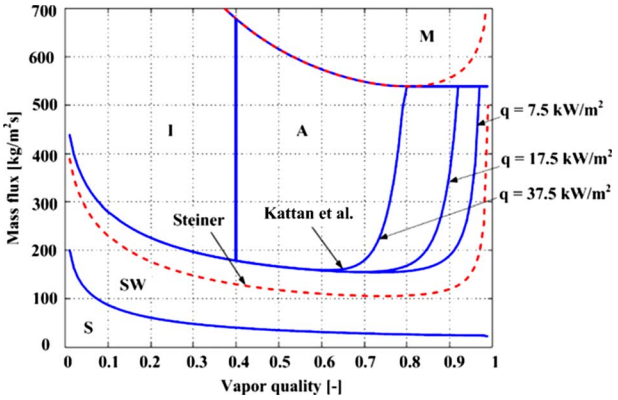

Fig. 9 The Kattan–Thome–Favrat flow-pattern map (solid lines) [10–12] compared to the Steiner map [9] (dashed lines) evaluated for R410A at T_{sat}=5°C in a 13.84 mm internal diameter tube at different heat fluxes [36]. (*A* stands for annular flow, *I* stands for intermittent flow, *M* stands for mist flow, *S* stands for stratified flow, and SW stands for stratified-wavy flow. The stratified to stratified-wavy flow transition is designated as *S*-SW, the stratified-wavy to intermittent/annular flow transition is designated as SW-*I*/*A*, the intermittent to annular flow transition is designated as *I*-*A*, and so on.)

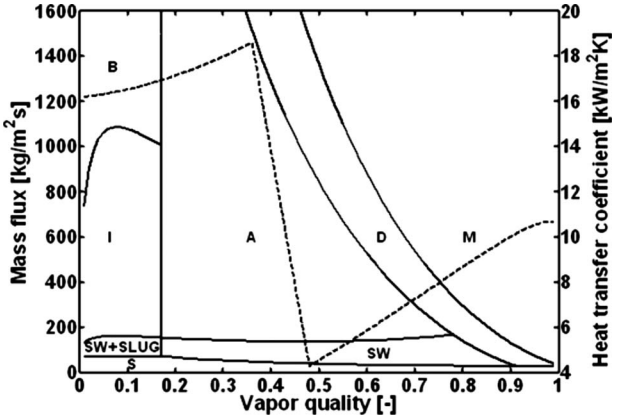

Fig. 11 The CO_2 flow-pattern map of Cheng et al. [22,23] evaluated for the test condition of Yun et al. [52]: D_{eq}=2 mm, G=1500 kg/m²s, T_{sat}=5°C, and q=30 kW/m² and the corresponding prediction of heat transfer coefficients (dashed line) (*B* stands for bubbly flow and others have the same meanings as in Figs. 9 and 10)

flow. The bubbly and mist flow transitions observed only at very high mass velocities were not verified in the map. Several new versions of the Kattan–Thome–Favrat diabatic map have been developed. Zürcher et al. [14] developed an updated version for horizontal flow boiling for R134a, R407C, and R717 (ammonia) for a wide range of mass velocities, vapor qualities, and heat fluxes. Thome and El Hajal [15] proposed a practical, easier to implement version of the flow map. Furthermore, El Hajal et al. [16] extended flow map to condensation of refrigerants (R22, R134a, R236ea, R125, R32, and R410A) inside horizontal channels, and Thome et al. [17] developed the corresponding flow-pattern-based condensation heat transfer model. Recently, Wojtan et al. [18,19] extended the Kattan–Thome–Favrat map to include a dryout region between the annular and mist flow regimes where dryout progresses around the tube perimeter from top to bottom, deduced by sharp changes in trends in their local heat transfer measurements for R22 and R410A. Figure 10 shows the flow-pattern map of Wojtan et al. [18,19] for R22 at the indicated conditions and the corresponding prediction of heat transfer. Thome and co-workers preferred to plot their maps in easy to use mass velocity G versus vapor quality x graphs calculated with the transition equations evaluated for the particular fluid, tube diameter, and heat flux. Such a format is much easier to use than nondimensional log-log maps.

Cheng et al. [20,21] developed a flow-pattern map for CO_2 evaporation inside horizontal tubes on the basis of the map of Wojtan et al. [18,19] by modifying the *I*-*A* and *A*-*D* boundary transitions. More recently, Cheng et al. [22,23] further modified the *A*-*D* boundary transition, proposed a new *D*-*M* boundary transition, added a bubbly flow-regime criterion (*B* stands for bubbly flow), and developed an updated flow boiling heat transfer model based on their flow map. Figure 11 shows the CO_2 flow-pattern map of Cheng et al. [22,23] evaluated for the indicated test conditions of Yun et al. [52] and the corresponding heat transfer prediction based on their map, which captured their data very well, as shown in Ref. [23].

A probabilistic two-phase flow-pattern map was first proposed by Niño [53] for refrigerant and air-water in multiport microchannels. Probabilistic flow maps have quality x on the X-axis and the

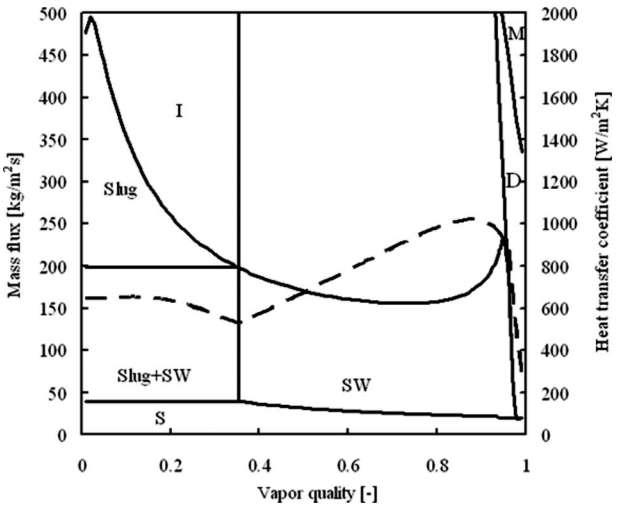

Fig. 10 The flow-pattern map of Wojtan et al. [18,19] for R22 at T_{sat}=5°C in a 13.84 mm internal diameter tube at G=100 kg/m²s and q=2.1 kW/m² and the corresponding prediction of heat transfer coefficients (dashed line) based on the map (*D* stands for the dryout region, slug stands for slug flow, and others have the same meanings as in Fig. 9)

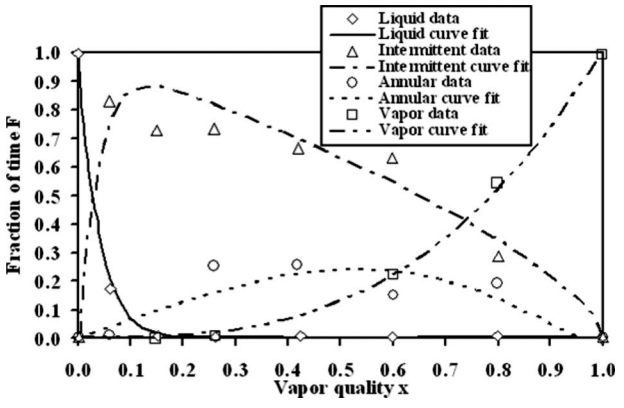

Fig. 12 The probabilistic flow map with time fraction curve fits for R134a at 10°C and a mass flux of 50 kg/m²s in a six-port microchannel (data obtained from Niño [53]) by Jassim and Newell [54]

fraction of time F in which a particular flow regime is obtained from processing videos taken at a given flow condition. Jassim and Newell [54] developed curve fit functions to represent the Niño [53] multiport microchannel time fraction data, which are continuous for the entire quality x range, as shown in Fig. 12. They then utilized the probabilistic flow map time fraction curve fits to predict pressure drops and void fractions, as will be discussed in Sec. 4. Furthermore, Jassim [55] and Jassim et al. [56] conducted experiments to obtain probabilistic two-phase flow map data for R134a and R410A in single smooth horizontal tubes including both macro- and microscale channels and extended the probabilistic flow map modeling techniques to single tubes. Jassim [55] developed curve fits of these probabilistic flow map data to generalize the time fraction information using physically meaningful parameters.

For all flow-pattern maps except the probabilistic type, it should be noted that the transitions between adjacent flow patterns do not actually occur suddenly but over a range of flow rate G or vapor quality x. Thus, the lines should really be replaced by rather broad transition bands. In addition, the majority of the flow-pattern maps have been developed for macroscale channels. The advantage of the probabilistic type map is that the flow transitions do not occur at a fixed location on the map but rather over a range of conditions that better reflect reality. However, so far it is not known how general such time fraction curve fits are. Presently, no generally accepted flow-pattern map for microscale channels is available, and an overall review on progress toward this goal is presented in the following section in addition to other cases.

3 Overall Review of the Studies of Flow Patterns and Flow-Pattern Maps

As there are a huge number of studies related to flow patterns and flow-pattern maps in the literature, the present paper does not include an exhaustive review but instead a summary of important aspects of flow patterns and flow-pattern maps. Both the experimental and theoretical studies are considered.

3.1 Experimental Studies. Various flow-pattern identification methods have been used in the experimental studies, including direct visual observation and observation through high speed photography or camera, x-ray absorption, multibeam gamma densitometry, signal processing of pressure fluctuations, void fraction fluctuations and light intensities, spectral distribution of wall pressure fluctuations, pressure gradient variations, neutron radiography, and electrical conductance probes [3,57–66], [140–142]. In this section, highlights of experimental studies on flow patterns and flow maps are summarized according to the following categories.

Studies on Macroscale Smooth Channels. A large number of experiments have been conducted with macroscale smooth channels over the past decades. These are mainly on gas-liquid flow structures and flow-regime transition criteria. Table 1 shows a summary of the principal studies of flow patterns in macroscale smooth channels, most of which are related to gas-liquid horizontal, vertical, and inclined upward cocurrent flows using air-water, air-other liquids, and refrigerant-refrigerant vapor as working fluids. Several studies are related to downward cocurrent flow and upward countercurrent flow. Direct visualization is the most often used method to identify flow regimes. Most researchers constructed flow maps or modified an available map, such as the Taitel–Dukler generalized flow map [7] based on their experimental data. It should be mentioned that most of these studies were conducted under adiabatic conditions. The studies of adiabatic gas-liquid two-phase flows are very helpful in understanding various flow regimes. However, flow maps developed for adiabatic flows cannot predict diabatic effects on flow-pattern transitions. For example, dryout from evaporation of an annular film in flow boiling does not exist in adiabatic two-phase flows. A diabatic flow map should include these effects and thus be useful to explain the corresponding heat transfer trends. Vice versa, sharp changes in heat transfer trends can in some cases be used to back out the corresponding flow-pattern transitions. Several such flow-pattern maps have been developed [10–23].

Studies on Microscale Channels. Studies on microscale channels have increased greatly in recent years. Ghiaasiaan and Abdel-Khalik [88] did a review of two-phase flow in microchannels and presented some published literature related to flow patterns in microscale channels with hydraulic diameters of the order of 0.1–1 mm. As mentioned in the Introduction, a distinction between macro- and microscale channels by the threshold diameter of 3 mm is adopted here. The principal microscale studies are presented in Table 2 according to this definition. Most studies used air-water or water-nitrogen as the working fluids for convenience. Some researchers used steam-water, nitrogen and its vapor, and refrigerants and their vapors such as R134a, CO_2, and R123. Both adiabatic and diabatic conditions have been investigated. Direct visualization was the most used identification method rather than a quantitative method. For example, Triplett et al. [47] conducted a systematic experimental investigation of air-water in microchannels with inner diameters of 1.1 mm and 1.45 mm for circular channels and with hydraulic diameters of 1.09 mm and 1.49 mm for semitriangular channels. The discernible flow patterns were bubbly, churn, slug, slug-annular, and annular flows, as shown in Fig. 13. Furthermore, they compared their results to the criteria of Suo and Griffith [89] and the mechanistic model of Taitel et al. [177] for the flow-pattern transition line leading to dispersed bubbly flow. The criteria of Suo and Griffith significantly disagreed with their data. The model of Taitel et al. [177] satisfactorily predicted the bubbly-slug transition line. However, transition from dispersed bubbly to churn flow was not captured. Figure 14 shows their observations compared with the experimental flow-pattern transition lines of Damianides and Westwater [101] taken for a circular 1 mm inner diameter test section. The flow-pattern names displayed on the figure represent the notation of Damianides and Westwater. The two data sets are in relative agreement with respect to slug and slug-annular flows (referred to as plug and slug, respectively, by Damianides and Westwater) and the flow conditions leading to annular flow.

Most researchers constructed their flow maps according to only their own experimental data. Hence these maps are only applicable to those specific conditions and fluids. Some researchers modified the generalized flow maps for macroscale such as the Taitel and Dukler map [7] or others according to their own data. Some researchers simply compared their flow-pattern data to the existing generalized flow maps for macroscale channels without further modifying these flow maps for microscale channels. Tabatabai and Faghri [121] proposed a new flow map to emphasize the importance of surface tension in two-phase flow in horizontal miniature and microtubes. In fact, their map is a modified version of the Taitel and Dukler [7] map that incorporates the surface tension effect on the flow-pattern transitions. So far, there is no independent experimental validation of observations for the same fluids under the same test conditions taken by different researchers.

In addition, the physical properties of fluids have a great effect on the flow regimes. For example, flow patterns of CO_2 at high reduced pressure are quite different from those of other refrigerants such as R22, R134a, and R410A. Thus, flow-pattern maps developed from these fluids do not extrapolate well to CO_2 [20–23,44]. Another example is that the flow-pattern map for helium is quite different from other fluids such as air-water and refrigerant as in Refs. [82,83]. In addition, microscale channels often have noncircular shapes, such as triangular, square, and rectangular, and may be single- or multichannel test sections, which greatly affect the flow regimes [38–44].

More recently, Ullmann and Brauner [122,123] studied the effect of the channel diameter on the mechanisms leading to flow-

Table 1 Summary of studies on flow patterns in macroscale smooth channels

Authors/References	Fluids, test channel diameter(s), and orientations	Main research contents	Remarks
Weisman and Kang [67]	(1) Air-water, circular tubes, 12 mm, 25 mm, and 51 mm; (2) air-glycerol, circular tube, 51 mm; (3) R113 evaporation, circular tube, 25 mm, inclined and horizontal.	Experimental study on flow-pattern transitions during gas-liquid two-phase flow in vertical and upwardly inclined channels. Development of improved dimensionless correlation for flow-pattern boundaries. The individual boundary lines have been combined into simple overall flow maps.	Adiabatic cocurrent flow.
Stanislav et al. [68]	Air-oil, circular tube, 25.8 mm, inclined.	Experimental measurements of flow patterns for intermittent flow in upward inclined pipes.	Adiabatic cocurrent flow.
Rozenblit et al. [69]	Air-aqueous surfactant solution, circular tube, 25 mm, vertical.	Flow-pattern observations and comparison of the experimental data with air-water flow map by Taitel and Dukler [7]. Good agreement has been reached.	Adiabatic cocurrent flow.
Furukawa and Fukano [70]	Air-water, air-aqueous glycerol, circular tube, 19.2 mm, vertical.	Visualization of flow patterns of gas-liquid flow. The effects of liquid viscosity on flow patterns were studied. The experimental data were compared to the Baker map [6]. The boundary between the bubbly flow and the slug flow cannot be captured.	Adiabatic cocurrent flow.
Zapke and Kröger [71]	Water, methanol, propanol, air, argon, helium, and hydrogen, rectangle ducts: heights of 50–150 mm and widths of 10–20 mm, an inclination angle of about 60 deg, near horizontal and vertical.	Three types of flow patterns depending on duct inclination: (1) roll waves at inclinations close to the horizontal, (2) a distinctive vortex-type flow at intermediate angles, and (3) churn-type flow containing elements of the vortex flow in the case of vertical ducts.	Adiabatic cocurrent flow.
Hasan and Kabir [72]	Air-water, annuli; outer diameter: 127 mm; inner diameters: 48 mm, 57 mm, and 87 mm; vertical and inclined annuli.	The experimental data were used to verify the prediction of the proposed methods of flow-pattern transitions and void fractions for bubbly, slug, and churn flow regimes.	Adiabatic cocurrent flow.
Govier and Short Leigh [73]	Air-water, circular tubes, 12.5 mm, 25 mm, 37.5 mm, and 50 mm, vertical.	The effect of channel diameter on flow patterns was studied.	Adiabatic cocurrent flow.
Crawford et al. [74,75]	R113 evaporation, circular tubes, 25 mm and 38 mm, vertical.	Observations of void fractions and flow patterns were made during steady-state cocurrent, downward flow.	Adiabatic cocurrent flow.
Weisman et al. [76]	Air-water and air-glycerol, circular tubes, 12 mm, 25 mm, and 51 mm, horizontal.	Transitions between flow patterns during cocurrent gas-liquid flow were experimentally studied. The effects of fluid properties and tube diameter were studied.	Adiabatic cocurrent flow.
Govier and Omer [77]	Air-water, circular tube, 25 mm, horizontal.	Experimental study of flow patterns was performed, and new data were obtained.	Adiabatic cocurrent flow.
Hand and Spedding [78]	Air-water, air and 78 wt % and 83 wt% glycerine water solution, circular tube, 93.5 mm, horizontal.	Flow patterns were experimentally studied. Theoretical and empirical flow maps were compared to the experimental data.	Adiabatic cocurrent flow.
Lin and Hanratty [79]	Air-water, circular tubes, 25.4 mm and 95.3 mm, horizontal.	Flow-patterns were experimentally studied. The effect of tube diameter on flow patterns was analyzed.	Adiabatic cocurrent flow.
Mukherjee and Brill [80]	Air-kerosene, air-lubricating oil, circular tube, 50.8 mm, inclined.	Flow-pattern data were experimentally obtained. Empirical equations for flow-pattern transitions were developed.	Adiabatic cocurrent flow.
Hashizume [81]	R12 and R22 evaporation, circular tube, 10 mm, horizontal.	Flow patterns were observed, and the experimental data were presented.	Adiabatic cocurrent flow.

Table 1 (***Continued.***)

Authors/References	Fluids, test channel diameter(s), and orientations	Main research contents	Remarks
Filippov [82]	Helium evaporation, circular tubes, 5.6 mm and 12 mm, annular channel: diameter of 13 mm and 11.1 mm, and rectangular slot: height of 30 mm and a gap of 1 mm, horizontal.	Flow patterns were experimentally studied. The experimental data were compared to the developed models. Good agreement was obtained.	Adiabatic cocurrent flow.
Alexeyev et al. [83]	Helium evaporation, circular tubes, 5.7 mm and 12 mm, rectangular slot: height of 30 and a gap of 1 mm, annular channel: diameter of 9 mm and a gap of 1 mm, horizontal.	Flow patterns were observed, and the experimental flow-pattern data are quite different from other two-phase mixtures.	Adiabatic cocurrent flow.
Barnea et al. [84]	Air-water, circular tubes, 19.5 mm and 25.5 mm, horizontal and inclined with an angle as large as 10 deg	Flow patterns were observed and the experimental data were compared to the Taitel and Dukler generalized flow map [7].	Adiabatic cocurrent flow.
Wolk et al. [85]	Air-water, circular, rectangular, rhombic, and equilateral triangular channels, 6 mm, vertical.	Flow patterns were experimentally studied and compared to the existing models.	Adiabatic cocurrent upward flow.
Ghajar [86]	Air-water, circular tube, 25.4 mm, horizontal and inclined with angles of about 2 deg, 5 deg, and 7 deg.	Flow patterns were observed and compared for various inclinations. Experimental data were shown on a flow map.	Adiabatic cocurrent (upward) flow.
Woldesemayat and Ghajar [87]	Natural gas-water, air-water, and air-kerosene, circular tubes, 12.7–102.26 mm, horizontal, vertical, and inclined with angles ranging from 5 deg to 80 deg.	Comparisons of 68 void fraction correlations to unbiased data set were made. An improved void fraction correlation that could acceptably handle all data sets regardless of flow patterns and inclination angles was suggested.	Adiabatic cocurrent (upward) flow.
Kattan et al. [10–12]	R134a, R123, R402A, R404A, and R502, evaporation, circular, 10.92 mm and 12 mm, horizontal.	Flow patterns were observed and related to the corresponding heat transfer prediction methods. A diabatic flow map was developed.	Diabatic cocurrent flow.
Zürcher et al. [14]	Ammonia evaporation, circular, 14 mm, horizontal.	Based on experimental data, a modified diabatic flow map of Kattan et al. [10–12] was developed.	Diabatic cocurrent flow.
Wojtan et al. [18,19]	R22 and R410A evaporation, circular, 8 mm and 13.84 mm, horizontal.	Flow patterns were observed and related to the corresponding heat transfer prediction methods. An improved diabatic flow map of Kattan et al. [10–12] was developed.	Diabatic cocurrent flow.
Cheng et al. [20–23]	CO_2 evaporation in horizontal tubes with a wide range of tube diameters of 0.6 to 10 mm (equivalent diameter D_e is used for non-circular channels).	A flow map was developed for CO_2 evaporation and flow-pattern-based heat transfer and pressure drop models were developed.	Diabatic cocurrent flow.

pattern transitions. They proposed mechanistic models for adiabatic conditions and compared these with experimental maps from the literature. Their models indicate the controlling dimensionless groups and the critical values associated with various flow-pattern transitions. By reducing the pipe diameter, the stratified flow region shrinks greatly and is limited to only a small region at very low liquid flow rates and relatively high gas flow rates. In the range where stratified flow may still exist, an analysis of the predicted flow structure indicates that the distinction between stratified flow (curved interface) and annular flow is ambiguous. From a practical point of view of the transport phenomena involved, the flow structure can be considered as annular flow. Figure 15 shows the comparison of the predicted flow-regime boundaries of the Ullmann and Brauner [122,123] flow map to the horizontal 1 mm tube experimental data of Triplett et al. [47]. High heat flux applications, such as cooling of microprocessors, bring in the onset of CHF (critical heat flux) through its corresponding critical vapor quality as an important flow-pattern map transition [124].

In the channel sizes of 0.01–3 mm, flow patterns can be different from those in macroscale channels. For example, the effect of channel orientation (vertical or horizontal) tends to disappear with

Table 2 Summary of studies on flow patterns in microscale channels

Authors/References	Fluids, test channel diameter(s), and orientations	Main research contents	Remarks
Alexeyev et al. [83]	Helium evaporation, rectangular slot with a gap of 1 mm, and annular channel with a gap of 1 mm, horizontal.	Experimental data of flow patterns for horizontal helium evaporation and flow maps were obtained.	Adiabatic cocurrent flow.
Ghiaasiaan and Abdel-Khalik [88]	Microscale channels with hydraulic diameters of the order of 0.1–1 mm.	Literature review on two-phase flow patterns and heat transfer in microscale channels.	Adiabatic and diabatic cocurrent flows.
Suo and Griffith [89]	Air-water, He, N_2/heptane, circular tube, 1 mm and 1.6 mm, horizontal.	Two-phase flow patterns were observed. Surface tension dominates over gravity.	Adiabatic cocurrent flow.
Revellin et al. [90]	R134a evaporation, circular tube, 0.5 mm, horizontal.	Flow patterns and transitions were identified by optical technique and observed by high speed video.	Diabatic cocurrent flow.
Revellin and Thome [91–93]	R134a and R245fa evaporation, circular tubes, 0.5 mm and 0.8 mm, horizontal.	Flow patterns were observed, and diabatic flow maps were proposed according to the experimental data.	Diabatic cocurrent flow.
Cubaud and Ho [94]	Air-water, square channels, 200×200 μm^2 and 525×525 μm^2.	Flow regimes were observed. A flow-pattern map and the transition lines between flow regimes were drawn for the microchannels.	Adiabatic cocurrent flow.
Coleman and Garimella [95]	Air-water, circular and rectangular channels, 5.5–1.3 mm, horizontal.	The effects of tube diameter and surface tension on flow patterns were experimentally studied.	Adiabatic cocurrent flow.
Chen and Garimella [96]	Dielectric fluid, multisquare channels, each 0.389×0.389 mm^2, horizontal.	Flow patterns were observed with high-speed visualizations.	Adiabatic cocurrent flow.
Zhao and Bi [97]	Air-water, equilateral triangular channels, hydraulic diameter D_h=5.5 mm, 2.886 mm, 1.443 mm, and 0.866 mm, vertical.	Flow patterns were observed, and the experimental data were compared to the flow-pattern models.	Adiabatic cocurrent flow.
Yun and Kim [98]	CO_2 evaporation, rectangular channel with a width of 16 mm and a height of 2 mm, horizontal.	Flow patterns were observed and compared to the existing flow maps. A flow map was proposed.	Adiabatic cocurrent flow.
Pettersen [99]	CO_2 evaporation, circular tube, 0.98 mm, horizontal.	Flow patterns were observed and flow maps were obtained.	Diabatic cocurrent flow.
Lowry and Kawaji [100]	Air-water, narrow passage between two flat plates with gaps: 0.5 mm, 1 mm, and 2 mm, vertical.	Flow patterns were studied, and flow maps were constructed based on the experimental data.	Adiabatic cocurrent upward flow.
Damianides and Westwater [101]	Air-water, compact heat exchanger with an equivalent diameter D_e=1.74 mm, several round tubes, 1 mm, 2 mm, 3 mm, 4 mm, and 5 mm, horizontal.	Flow patterns were determined by high-speed photography and fast-response pressure transducers. Flow maps were constructed.	Adiabatic cocurrent flow.
Yang and Shieh [102]	Air-water, R134a evaporation, circular tube, 1–3 mm, horizontal.	Flow patterns were studied, and the experimental data were compared to the available models.	Adiabatic cocurrent flow.
Huh and Kim [103]	Water evaporation, rectangular channels, hydraulic diameter D_h=0.1035 mm and 0.133 mm, horizontal.	Real time flow visualization of the phase change process was performed.	Diabatic cocurrent flow
Hardt et al. [104]	2-propanol and water evaporation, multisquare channels: 0.05×0.05 mm^2, 0.03×0.03 mm^2, horizontal.	Flow patterns were visualized during evaporation processes.	Diabatic cocurrent flow.
Owhaib et al. [105]	R134a evaporation, circular tube, 1.33 mm, vertical.	The flow patterns at high vapor qualities and the dryout of the liquid film were visually studied.	Diabatic cocurrent flow.

Table 2 (***Continued.***)

Authors/References	Fluids, test channel diameter(s), and orientations	Main research contents	Remarks
Sobierska et al. [106]	Steam-water, rectangular hydraulic diameter D_h=1.2 mm, vertical.	Flow patterns were studied and compared to the existing criteria.	Diabatic cocurrent flow.
Yen et al. [107]	R123 evaporation, circular channel, 0.21 mm and square channel, 0.214 mm, horizontal.	Visualizations of flow patterns with simultaneous measurement of heat transfer coefficients were performed.	Diabatic cocurrent flow.
Ekberg et al. [108]	Air-water, annuli with a gap of 2 mm, horizontal.	Flow patterns were studied and flow maps were constructed.	Adiabatic cocurrent flow.
Fukano et al. [109]	Air-water, circular tubes, 1 mm, 2.4 mm, and 4.9 mm, horizontal.	Flow patterns were studied and flow maps were constructed.	Adiabatic cocurrent flow.
Serizawa et al. [110]	Air-water, steam-water, circular tubes, 0.02 mm, 0.025 mm, 0.05 mm, and 0.1 mm, horizontal.	Flow patterns were observed and a flow map was constructed.	Adiabatic cocurrent flow.
Ide et al. [111]	Air-water, circular tubes, 1 mm, 2.4 mm, and 4.9 mm, rectangular, 1×1 mm^2, 2×1 mm^2, 5×1 mm^2, and 9.9×1.1 mm^2, vertical upward and downward, and horizontal.	The effects of the tube diameters and aspect ratios of the channels on flow patterns were studied.	Adiabatic cocurrent flow.
Satitchaicharoen and Wongwises [112]	Air-water, air–20 wt % and 40 wt % glycerol, rectangular channels hydraulic diameter D_h=1.95 mm, 3.81 mm, 5.58 mm, 3.63 mm, and 3.87 mm, vertical.	The effects of channel gap sizes, channel widths, and liquid viscosities on flow-pattern transitions were studied.	Adiabatic cocurrent flow.
Li and Peterson [113]	Steam-water, rectangle channel with a hydraulic diameter D_h=0.056 mm, horizontal.	Flow patterns were observed during boiling process.	Diabatic cocurrent flow.
Barajas and Panton [114]	Air-water, circular tube, 1.6 mm, horizontal.	The effects of contact angle on flow patterns were studied.	Adiabatic cocurrent flow.
Hetsroni et al. [115]	Air-water, water-steam, multitriangular channels, hydraulic diameter D_h=0.129 mm, 0.103 mm, and 0.161 mm, horizontal.	Flow patterns were experimentally studied for both adiabatic and diabatic conditions.	Adiabatic and diabatic cocurrent flows.
Kawahara et al. [116]	Water-nitrogen, circular channels, 0.1 mm, horizontal.	Flow patterns were observed, and a flow map was constructed and compared to the existing flow map.	Adiabatic cocurrent flow.
Chung and Kawaji [117]	Water-nitrogen, circular channels, 0.53 mm, 0.25 mm, 0.1 mm, and 0.05 mm, horizontal.	Flow patterns were observed, and the effect of channel diameter on flow patterns was studied.	Adiabatic cocurrent flow.
Nakoryakov et al. [118]	Air-water, concentric annular channel with a gap of 0.68 mm gap, vertical.	Flow patterns were experimentally studied and a flow map was constructed.	Adiabatic cocurrent flow.
Fukano and Kariyasaki [119]	Air-water, circular tubes, 1 mm, 2.4 mm, and 4.9 mm, vertical upward and downward, horizontal.	Flow patterns were experimentally studied and flow maps were constructed.	Adiabatic cocurrent flow.
Wambsganss et al. [120]	Air-water, rectangular channel 19.05×3.18 mm^2, horizontal.	Flow patterns were studied and flow maps were constructed.	Adiabatic cocurrent flow.
Triplett et al. [47]	Air-water, circular channels, 1.1 mm and 1.45 mm, semitriangular channels with hydraulic diameter D_h=1.09 mm and 1.49 mm, horizontal.	Flow patterns were studied. The experimental data were compared to the existing data and flow maps.	Adiabatic cocurrent flow.
Brauner and Moalem-Maron [48]	Theoretical analysis on microscale channel criterion.	Theoretical analysis of the identification of the range of small diameter channels related to flow-pattern transitions.	Adiabatic and diabatic cocurrent flows.
Tabatabai and Faghri [121]	Modeling of flow regimes in horizontal small tubes.	A new flow map accounting for surface tension effects was proposed.	Adiabatic cocurrent flow.

Table 2 (*Continued.*)

Authors/References	Fluids, test channel diameter(s), and orientations	Main research contents	Remarks
Cheng et al. [20–23]	CO_2 evaporation in horizontal tubes with a wide range of tube diameters of 0.6–10 mm (an equivalent diameter D_e is used for noncircular channels).	Flow-pattern map was developed for CO_2 evaporation. Flow-pattern-based heat transfer and pressure drop models were developed.	Diabatic cocurrent flow.
Niño [53], Jassim and Newell [54], Jassim [55], and Jassim et al. [56]	Modeling of flow regimes.	Probabilistic flow-pattern maps were proposed based on experimental data.	Adiabatic cocurrent flow.
Ullmann and Brauner [122,123]	Prediction of flow regimes in mini channels.	Appropriate mechanistic models were proposed.	Adiabatic cocurrent flow.

decreasing channel size. New flow patterns, such as wedge flow [94] and liquid lump flow [110], appear. Slug flows have much longer bubbles, reaching length to channel diameter ratios of 10–100 [90–93].

Cubaud and Ho [94] studied air-water flows in 200 $\times 200\ \mu m^2$ and $525 \times 525\ \mu m^2$ square microchannels made of glass and silicon and observed bubbly flow, wedge flow, slug flow, annular flow, and dry flow. The newly defined wedge flow was proposed. As shown in Fig. 16, wedge flow consists of elongated bubbles, the size of which d is larger than the channel width h with partial dryout of the film at the center of the walls downstream from the nose of the bubble. Wedge flow exhibits some differences from the Taylor bubbly flow. For a partially wetting system, as a function of the bubble velocity, the perimeter of the bubbles can dry out at the center face of the channel creating triple lines (liquid-gas-solid) while liquid still flows in the corners.

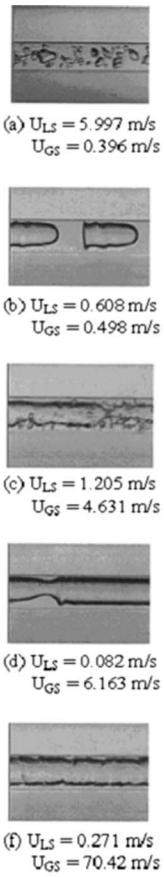

(a) Bubbly; (b) Slug flow; (c)Chum flow; (d) Slug-annular flow; (f) Annular flow.

Fig. 13 Photographs of flow patterns in a 1.1 mm diameter test section of Triplett et al. [47]

Similar to the case in macroscale channels, flow patterns at adiabatic conditions are different from those at diabatic conditions in microscale channels. Diabatic flows have been studied by several researchers. Flow patterns in a 0.509 mm microchannel for R245fa at 35°C and 500 $kg/m^2 s$ observed by Revellin and Thome [91–93] are shown in Fig. 17. Several transition regimes such as bubbly/slug flow, slug/semiannular flow, and semiannular flow have been defined according to their observations, the latter of which probably coincides with churn flow in macroscale channels. Figure 18 shows their diabatic flow-pattern map observations and boundaries for R134a [91,92]. Based on only data in one or two channels and one fluid, such flow maps are not applicable to other fluids and test conditions.

In general, the study of flow patterns in microscale channels is still in its infancy. Well documented theoretically based flow-pattern transition criteria and flow maps for microscale channels have not yet been established. Further efforts should be made to develop a generalized flow map for microchannels, which may be applied to a wide range of conditions and fluids.

Studies on Tube Bundles. Flow patterns in tube bundles are important for the design of evaporators and condensers. Table 3 shows a summary of studies on tube bundles. Both horizontal and vertical bundles with upward and downward flows are concerned. Some researchers used air-water to investigate the flow patterns in tube bundles, while several studies used diabatic vapor-liquid flows. Figure 19 shows the proposed flow-pattern categories for a tube bundle: (a) bubbly, (b) intermittent, (c) annular, (d) stratified, (e) stratified spray (from Grant and Chisholm [135]), and (f) intermittent downward flows, (g) falling film, and (h) churn flow from Xu et al. [134]. Casciaro and Thome [127,128] presented a comprehensive review of heat transfer, void fraction, two-phase pressure drops, and flow patterns in flooded evaporators. Ribatski and Thome [125,126] recently reviewed two-phase flow and flow boiling across horizontal tube bundles. They summarized the heat transfer mechanisms related to flow patterns, where more information may be obtained in Refs. [125,126]. For tube bundles, no proven generalized flow-pattern map is yet available as the two-phase flows are quite complex. The most widely quoted flow map is that of Grant and Chisholm [135].

Studies on Condensation in Tubes. Condensation inside channels is an important industrial process. Table 4 presents a summary of flow-pattern studies during condensation in tubes. All these studies are related to condensation inside horizontal tubes with various fluids such as steam, *N*-pentane, and refrigerants. Both macro- and microchannels are included. Usually, direct visualization has been used to classify the flow structures during

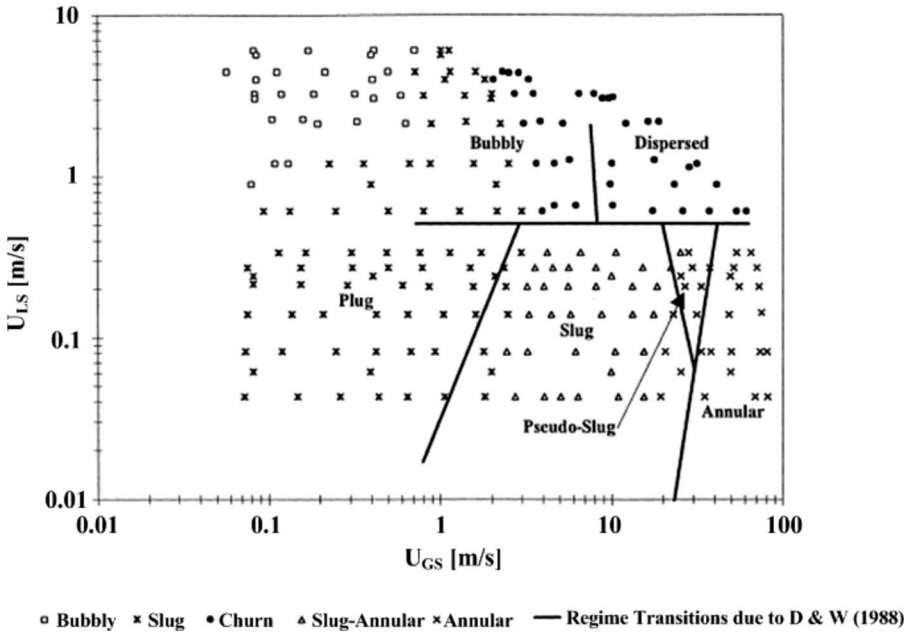

Fig. 14 Comparison between the experimental flow patterns observed by Triplett et al. [47] for a 1.1 mm diameter circular test section to the experimental flow-regime transition lines of Damianides and Westwater [101] based on a 1 mm diameter circular test section

condensation. Some researchers simply compared their data to the available adiabatic maps or constructed flow maps according to their experimental data. Apparently such flow maps lack a generalized character and are difficult to apply to other conditions or fluids.

Palen et al. [49] studied the prediction of flow regimes during condensation in horizontal tubes. They classified them into two basic regimes: shear-controlled flow, in which the condensation mechanism is of forced convection type, and gravity-controlled flow, in which the condensation mechanism is the Nusselt type. They described the basic flow regimes during condensation in horizontal tubes, as shown in Fig. 5. They also pointed out that the prediction of flow regimes was crucial for an accurate estimation of heat transfer coefficients during condensation in tubes. A visual investigation of condensation in a horizontal glass tube indicated that the Baker [6] flow-regime map did not provide a realistic picture of controlling regimes in condensation. They proposed a new approach based on simple force ratios, which greatly improved the prediction for all existing data.

Coleman and Garimella [144] conducted a comprehensive experimental investigation of the two-phase flow mechanisms during the condensation of R134a in six circular, square, and rectangular channels covering both macro- and microscale dimensions. The flow mechanisms were categorized into four principal flow

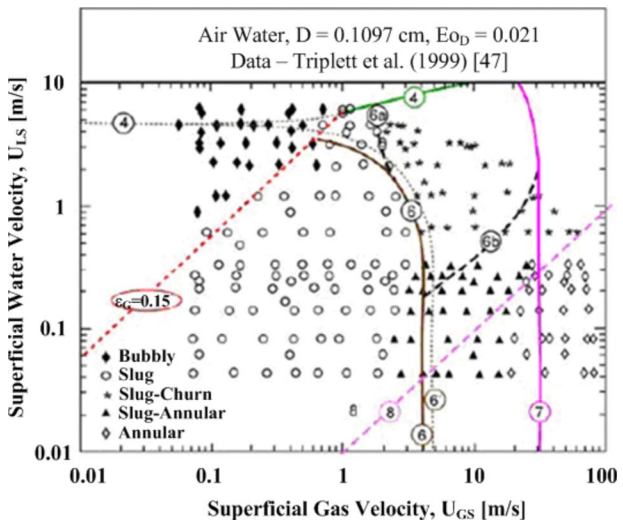

Fig. 15 Comparison of the predicted flow-regime boundaries of the Ullmann and Brauner [122,123] flow map in a horizontal 1 mm tube to the experimental data of Triplett et al. [47], where ε_G is the cross-sectional void fraction and Eo_D is the Eotvös number

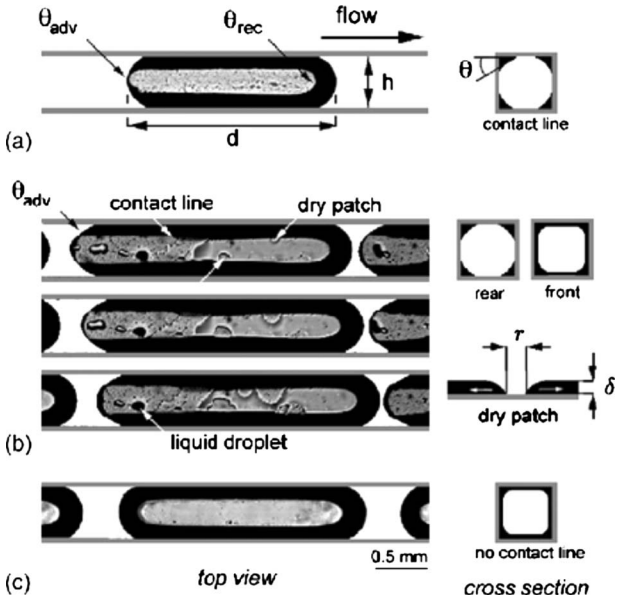

Fig. 16 Wedge flow regime: (*a*) drying bubble, (*b*) consecutive images of a hybrid bubble, and (*c*) lubricated bubble, observed by Cubaud and Ho [94]

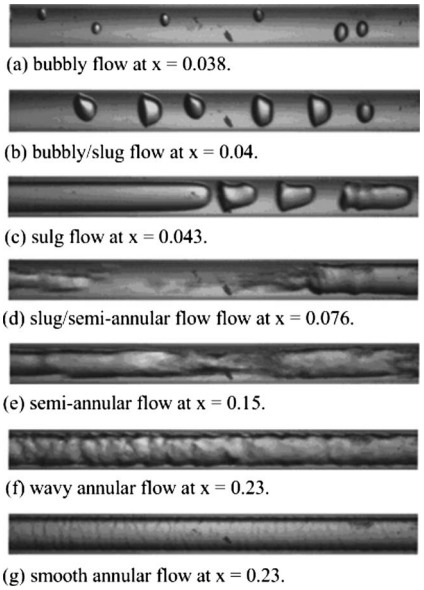

Fig. 17 Flow patterns in a 0.509 mm microchannel for R245fa at 35°C and 500 kg/m² s, observed by Revellin and Thome [90–92] at the exit of a microevaporator channel

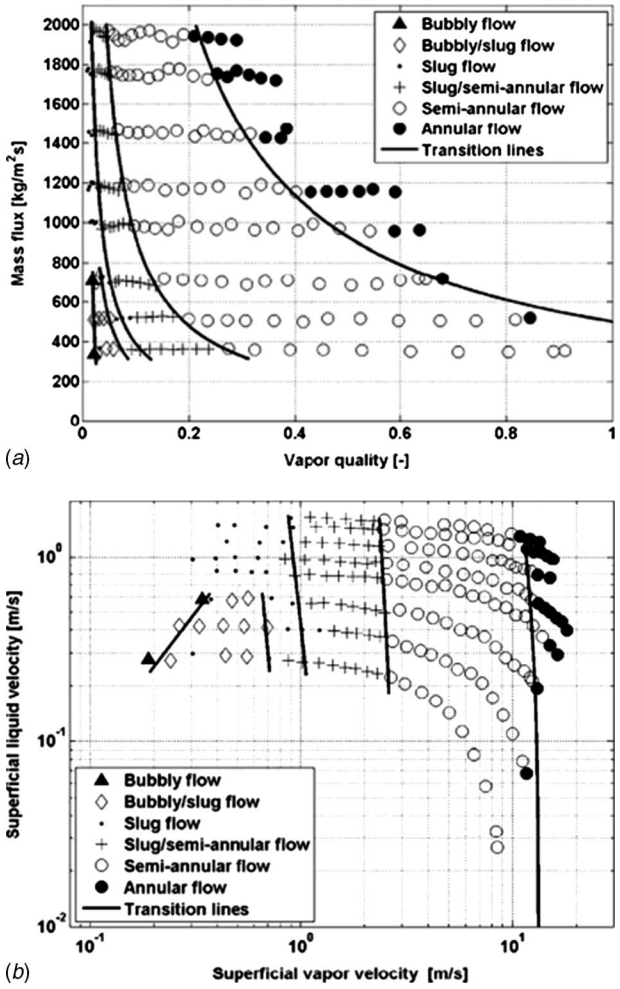

Fig. 18 Flow-pattern observations With experimental transition lines for R134a, D=0.5 mm, L=70.7 mm, T_{sat}=35°C and ΔT_{sub}=5°C using laser plotted in two different formats: (*a*) flow-pattern observations with transition lines and (*b*) flow-pattern map by Revellin and Thome [91,92].

regimes: intermittent flow, wavy flow, annular flow, and dispersed flow. Transition lines between the respective flow patterns and regimes on these maps were established based on the experimental data. Figure 20 shows the map for R134a condensing in a 4.91 mm circular tube. The annular, wavy, and intermittent regimes are present in this tube. A major portion of this map is occupied by the wavy flow regime with a small region where the plug, slug, and discrete wave flow patterns coexist. Both discrete and disperse wave patterns are present, with the waves becoming increasingly dispersed as the quality and mass flux are increased (shown by the arrow in Fig. 20). It was found that for similar hydraulic diameters, flow-regime transitions are not dependent on tube shape or aspect ratio. These flow maps and the transition lines can be used to predict the particular flow pattern or regime that will be established for a given mass flux, quality, and tube geometry.

Like that in flow boiling or evaporation, it is very important to relate the two-phase flow patterns to the corresponding heat transfer phenomena and mechanisms. In this aspect, El Hajal et al. [16] proposed a flow-pattern map for condensation based on a number of experimental data of various refrigerants, and Thome et al. [17] applied their flow-pattern map to the prediction of condensation heat transfer coefficients after a comprehensive review of the available adiabatic maps, which is developed similar to the flow-pattern-based flow boiling heat transfer method of Kattan et al. [10–12] mentioned earlier. Their model includes the effect of flow regime, stratification, and interfacial waves on heat transfer.

Liebenberg et al. [136] and Liebenberg and Meyer [137] conducted experimental studies on flow regimes during the condensation of refrigerants in horizontal smooth and microfin tubes. The power spectral density distribution of the fluctuating condensing pressure signal was used to identify the prevailing flow regimes, as opposed to the traditional (and subjective) use of visual-only methods. The flow-pattern data were compared to the flow map of El Hajal et al. [16]. For their smooth tube, the map of El Hajal et al. worked well. Figure 21 shows the video images of condensing R-134a at 300 kg/m² s, 500 kg/m² s, and 800 kg/m² s in their smooth tubes, superimposed on the map of El Hajal et al. [136]. The flow regimes observed for microfin tubes were similar to those for smooth tube condensation, except that the transition from annular to intermittent flow occurred at lower vapor qualities compared to those for smooth tube condensation [138].

It should be pointed out that condensation in microscale channels is of great interest in a wide range of applications. However, so far, only a few studies on flow patterns and flow-pattern maps for microscale channels are available [139–141,143,144]. Systematic experiments are needed to contribute to the knowledge of flow patterns and flow maps in microscale channels in the future.

Furthermore, as an important condensation mode, the study of dropwise condensation should be mentioned here as well [145] although only a few studies concern this topic. Cheng and van der Geld [146] and Cheng et al. [147] observed dropwise condensation phenomena of air-steam flow in a compact polymer heat exchanger made of polyvinylidene-fluoride (PVDF). Dropwise condensation was achieved on the heat transfer surfaces. The liquid drops were broken into very small liquid droplets due to the high gas-liquid shear stress caused by very high air flow velocities. Thus, the flow regimes during dropwise condensation are air dropwise-liquid flow, air dropwise-film liquid flow, droplet dispersed flow, and mist flow.

Overall, few flow-pattern data for condensing conditions are available so far. Therefore, more studies of condensation inside tubes should be conducted. Emphasis should be given to research using quantitative flow-pattern identification techniques and to the study of flow patterns and flow maps in microscale channels as well. In general, additional work in condensation flow-regime pre-

Table 3 Summary of studies on flow patterns across tube bundles

Authors/References	Fluids and test section positions	Main research contents	Remarks
Ribatski and Thome [125,126]	Two-phase flow and flow boiling across horizontal tube bundles, upward, downward, and side-to-side flows.	A state-of-the-art review of two-phase flow and flow boiling across horizontal tube bundles.	Adiabatic and diabatic cocurrent flows.
Casciaro and Thome [127,128]	Two-phase flow and heat transfer in flooded evaporators.	Review of boiling heat transfer, void fraction, two-phase flow pressure drop, and flow-pattern studies.	Adiabatic and diabatic cocurrent flows.
Venkateswararao et al. [129]	Air-water, two-phase flow up along the vertical rod bundle.	Flow patterns were experimentally and analytically studied.	Adiabatic cocurrent flows.
Aprin et al. [130]	*N*-pentane, propane, and isobutane evaporation, vertical upward flow boiling across the horizontal tube bundle.	Flow patterns were observed and a flow-pattern map was proposed.	Diabatic cocurrent flow.
Narrow et al. [131]	Air-water, two-phase along the microrod bundle.	Flow patterns were observed and flow-pattern transition lines were empirically correlated.	Adiabatic cocurrent flow.
Ulbrich and Mewes [132]	Air-water, two-phase flow up and down across the horizontal tube bundle.	Flow patterns were obtained. A general flow-pattern map was proposed.	Adiabatic cocurrent flow.
Noghrehkar et al. [133]	Air-water, vertical upward flow boiling across the horizontal tube bundle.	A resistivity void probe was used to measure the local void fraction, and the probability density function (PDF) of local void fraction fluctuations was used in an objective statistical method to determine flow regimes.	Adiabatic cocurrent flow.
Xu et al. [134]	Air-water, two-phase flow up and down across the horizontal tube bundle.	Flow patterns were obtained in the cross flow zones and flow-pattern maps were constructed.	Adiabatic cocurrent flow.
Grant and Chisholm [135]	Air-water, flow patterns, and pressure drops in a shell-and-tube heat exchanger.	Flow patterns were observed on the shell side of the heat exchanger.	Adiabatic cocurrent flow.

diction covering a wider range of fluids (including mixtures and noncondensables) and tube geometries appears to be necessary if further real improvement on condensation heat transfer prediction is to be accomplished.

Studies Under Microgravity Conditions. Studies under microgravity conditions have emerged in the past few years. Due to the anticipated high-power-level demands for thermal management in future spacecraft and aboard the Space Station Freedom, active methods of transporting heat along a spacecraft are being pursued. Table 5 presents a summary of the studies under microgravity conditions. Due to the effect of gravity, available flow-pattern maps under gravity conditions surely cannot predict the flow patterns under microgravity conditions. Various flow-pattern transitions and flow maps were proposed according to the experimental data under microgravity conditions. For example, Rezkallah [152] reviewed the studies of flow patterns under microgravity and also proposed a Weber number based flow map, which considered the effect of surface tension. Bousman et al. [154] proposed a flow map for microgravity conditions according to their experimental data. Zhao et al. [155] compared their flow-pattern data under microgravity conditions to the existing flow-pattern models without further proposing flow-pattern transition criteria for their observations. Celata et al. [156] recently conducted an experimental study of flow boiling of FC-72 under microgravity and normal gravity conditions with simultaneous observations in their glass heated test section. They proposed a modification of the flow map of Colin et al. [150].

Ohta [157] did a review of microgravity heat transfer in flow boiling and showed some photos of flow regimes under microgravity conditions. As his review focused on flow boiling heat transfer, no systematic discussion of flow patterns in flow boiling under microgravity was presented. Apparently, no flow-pattern study on condensation under microgravity conditions has been performed so far. Therefore, future studies should consider the effects of flow pattern during both flow boiling and condensation under microgravity conditions, especially for microscale channels.

Studies on Complex Channels. Studies of flow patterns in complex structured channels such as various enhanced heat transfer tubes, U-bends, coiled tubes, and diverging and converging channels are also very important in practical applications but have been seldom conducted so far. For example, a number of studies on flow boiling heat transfer inside enhanced tubes have been done [158–162]. However, little information on flow patterns in these enhanced tubes is available. Table 6 presents a selection of studies on flow patterns in complex channels. All these studies are related to adiabatic gas-liquid two-phase flows. It seems that no study was conducted under diabatic conditions so far. The reason is possibly due to the difficulty in observing the flow patterns in

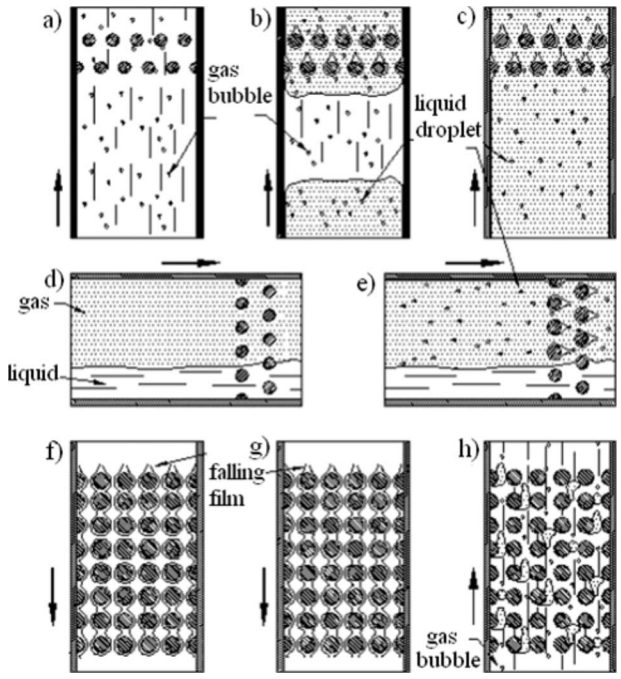

Fig. 19 Proposed flow-pattern categories in two-phase flow across a tube bundle: (*a*) bubbly, (*b*) intermittent, (*c*) annular, (*d*) stratified, (*e*) stratified-spray from Grant and Chisholm [135], and (*f*) intermittent downward flows, (*g*) falling film and (*h*) churn from Xu et al. [134] shown by Ribatski and Thome in Refs. [125,126].

the complex tube structures under diabatic conditions. Generally, the available studies for adiabatic flows have provided some fundamental information specific to the complex channels in question, but no general approach for dealing with all these geometries seems available. It should be mentioned that flow patterns in rod bundle channels are very important in nuclear power engineering and have gained significant attention. Although a number of studies of flow boiling heat transfer in such channels have been conducted [173], few studies of flow regimes under diabatic conditions have been found. Therefore, in the future, investigation on flow patterns in complex channels should be done under diabatic conditions (flow boiling and condensation). Furthermore, flow patterns should be related to the corresponding heat transfer and pressure drop characteristics. Efforts should be made to develop flow-pattern-based heat transfer and pressure drop models for complex channels.

Studies of Highly Viscous Newtonian Fluids. For highly viscous Newtonian liquids (non-Newtonian fluids are beyond the scope of the present review due to their different rheology such as inconstant viscosity); flow patterns like those in Fig. 22 are observed by Dziubinski et al. [175]. The difference between these flow patterns and those for normal Newtonian fluids is in the flow structures. For example, a bubble may become larger in a highly viscous Newtonian bubbly flow due to the effect of viscosity on the liquid and gas velocities. There is very little research on highly viscous Newtonian gas-liquid flows. Just to mention two studies, one study is for horizontal tubes by Chhabra and Richardson [174], and the other one is for a vertical tube by Dziubinski et al. (175). These studies have provided a good starting point for further work on these topics. Further extensive experiments should be done over a wide range of conditions to develop a generalized flow map for highly viscous Newtonian fluids.

3.2 Theoretical Studies. Theoretical studies mainly address the modeling of flow-regime transitions and hydrodynamic models for dispersed bubbly flow, stratified flow, stratified-wavy flow, slug flow, intermittent flow, annular-flow, annular dispersed liquid flow, mist flow, and flow instabilities. They generally provide a theoretical insight into understanding various aspects of two-phase phenomena.

Modeling of Flow-Regime Transitions. As aforementioned, perhaps the most comprehensive treatment of flow-regime transitions on a semitheoretical basis is that of Taitel and Dukler [7] for gas-liquid two-phase flow. The mechanisms for flow-regime transitions are based on physical concepts. The flow regimes are intermittent (slug and plug), stratified smooth, stratified wavy, dispersed bubble, annular, and annular dispersed. The theory predicts the influence of tube size, fluid properties, and angle of inclination. A generalized flow-regime map based on this theory was developed as shown in Fig. 8 for horizontal flows. Based on this work, Taitel et al. [176,177] conducted several studies on flow patterns theoretically. One example is the theory for predicting flow-pattern transition under transient flow conditions [176]. This work represents an extension of their methods for steady state flows. Under transient conditions, flow-pattern transitions can take place at flow rates substantially different than what would occur under steady conditions. In addition, flow patterns can change much more than one would expect for a slow change in flow rate along the same path. They also developed models for predicting flow-pattern transitions during steady gas-liquid flow in vertical tubes based on physical mechanisms suggested for each transition [177]. These models incorporate the effect of fluid properties and pipe size and are thus largely free of the limitations of empirically based transition maps. Models are developed to predict the transition boundaries between the four basic flow patterns for gas-liquid flow in vertical tubes: bubble, slug, churn, and dispersed annular. It is suggested that churn flow is the development region for the slug pattern and that bubble flow can exist in small pipes only at high liquid flow rates, where turbulent dispersion forces are high. Each transition is shown to depend on the respective flow rates of the phases, fluid properties, and pipe size, but the nature of the dependence is different for each transition because of differing controlling mechanisms. The theoretical predictions are in reasonably good agreement with a variety of published flow maps based on experimental data.

Other flow-pattern transition models have been proposed by Weisman et al. [76], Weisman and Kang [67], Taitel and Barnea [178], Ito et al. [179], and Crawford and Weisman [180]. It has been recognized that the controlling dimensionless correlating groups varied from transition to transition and obtained separate correlations for each transition in these studies. Crawford and Weisman [180] found that the flow-pattern map developed for adiabatic round tube data, which was used in their study, was generally in reasonable agreement with diabatic data and data in noncircular ducts. With the allowance for the annular transition being somewhat below predictions in small channels, the map appears to provide reasonable flow-pattern predictions at moderate pressures. For the most part, the observed deviations are within the scatter inherent in flow-pattern observations.

McQuillan and Whalley [181] presented a model for two-phase flow patterns in vertical channels, which included the transition between plug flow and churn flow under the assumption that flooding of the falling film limits the stability of plug flow. The resulting equation is combined with other flow-pattern transition equations to produce a theoretical flow-pattern map. The map was compared to flow-pattern observations, and encouraging agreement was obtained. Bilicki and Kestin [182] proposed three simple models and used them to determine, semiheuristically, the transition criteria from bubble to slug flow and from slug to froth flow. Their results for flow patterns agreed well with those of Taitel et al. [177].

Mishima and Ishii [183] studied flow transitions for upward two-phase flow in vertical tubes according to a two-fluid model. For a two-fluid model, direct geometrical parameters such as the void fraction should be used in flow-regime criteria. From this

Table 4 Summary of studies on flow patterns during condensation

Authors/References	Fluids and test section positions	Main research contents	Remarks
Liebenberg et al. [136] and Liebenberg and Meyer [137]	R22, R407C, and R134a, smooth and microfin tubes, 8.11 mm, 9.081 mm, 8.936 mm, and 8.668 mm, horizontal.	The power spectral density (PSD) distribution of the fluctuating condensing pressure signal was used to identify the flow regimes.	Diabatic cocurrent flow.
Olivier et al. [138]	R22, R407C, and R134a, smooth, helical microfin, and herringbone tubes, horizontal.	Flow regimes were observed. New flow-pattern transitions were proposed.	Diabatic cocurrent flow.
Louahlia-Gualous and Mecheri [139]	Steam, circular tube, 0.78 mm, horizontal.	Visualization and experimental measurements of condensation flow patterns were studied.	Diabatic cocurrent flow.
Mederic et al. [140,141]	*N*-pentane, circular tubes, 10 mm, 1.1 mm, and 0.56 mm, horizontal.	The effects of channel diameter on the condensation flow patterns were studied.	Diabatic cocurrent flow.
Chen et al. [142]	R134a, 3D microfin tubes with inner diameter inside diameter D_i=12 mm and 14 mm, horizontal.	Flow patterns were experimentally studied and compared to models.	Diabatic cocurrent flow.
Chen and Cheng [143]	Steam, microparallel channels, hydraulic diameter D_h=0.075 mm, horizontal.	A visualization study of condensation was performed.	Diabatic cocurrent flow.
Coleman and Garimella [144]	R134a, round, square, and rectangular channels, hydraulic diameter D_h=4.91 mm, 4 mm, 4.8 mm, and 2.67 mm, horizontal.	Flow patterns were experimentally studied and flow maps were constructed.	Diabatic cocurrent flow.
El Hajal et al. [16] and Thome et al. [17]	R22, R134a, R410a, R125, R32, and R236fa, circular tube, 8 mm, horizontal.	A new flow-pattern map that is related to condensation heat transfer was developed for condensation.	Diabatic cocurrent flow.
Cheng and Van der Geld [146] and Cheng et al. [147]	Air-steam mixtures, a polymer compact (PVDF) heat exchanger of 46 narrow parallel flow channels with a gap of 2 mm.	Dropwise condensation was achieved on the PVDF surfaces. Flow patterns were visualized during the condensation process.	Diabatic cocurrent flow.

point of view, new flow-regime criteria have been developed for a vertical upward flow. These criteria have been compared with the conventional criteria and experimental data for atmospheric pressure air-water flows and high pressure steam-water flows in round tubes and a rectangular channel. Considering the different methods of observations, definitions of the flow regimes and the transition phenomena themselves, which develop gradually, they concluded that their criteria showed satisfactory agreements with those data. Recently, Hibiki and Mishima [184] extended the Mishima–Ishii model [183] to vertical upward flows in narrow rectangular channels and developed new flow-regime transition criteria. These new criteria have been compared with the existing experimental data for air-water flows in narrow rectangular channels with gaps of 0.3–17 mm and showed satisfactory agreement. Further comparisons to steam-water data in a rectangular channel at relatively high system pressures were also successful. These results confirmed that their flow-regime transition criteria could be applied over wide ranges of parameters, as well as to boiling flow. For microscale channels, this last model may be a good starting point.

Barnea [185] summarized models for predicting flow-pattern transitions in steady gas-liquid flow in pipes and presented models that incorporate the effect of fluid properties, pipe size, and angle of inclination in a unified way that is not restricted to a specific range of pipe inclinations. She also presented flow-pattern transition mechanisms for each individual boundary and a logical path for a systematic determination of the flow patterns. This is par-

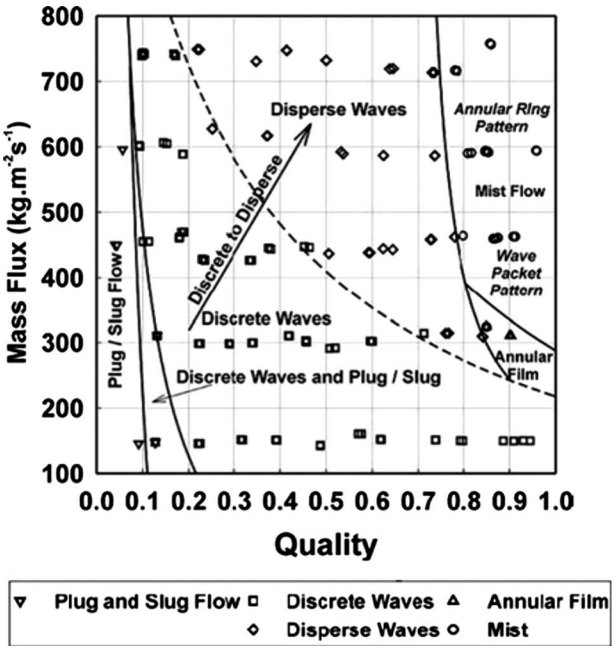

Fig. 20 The Coleman and Garimella [144] flow-regime map for R134a condensation in a 4.91 mm circular tube

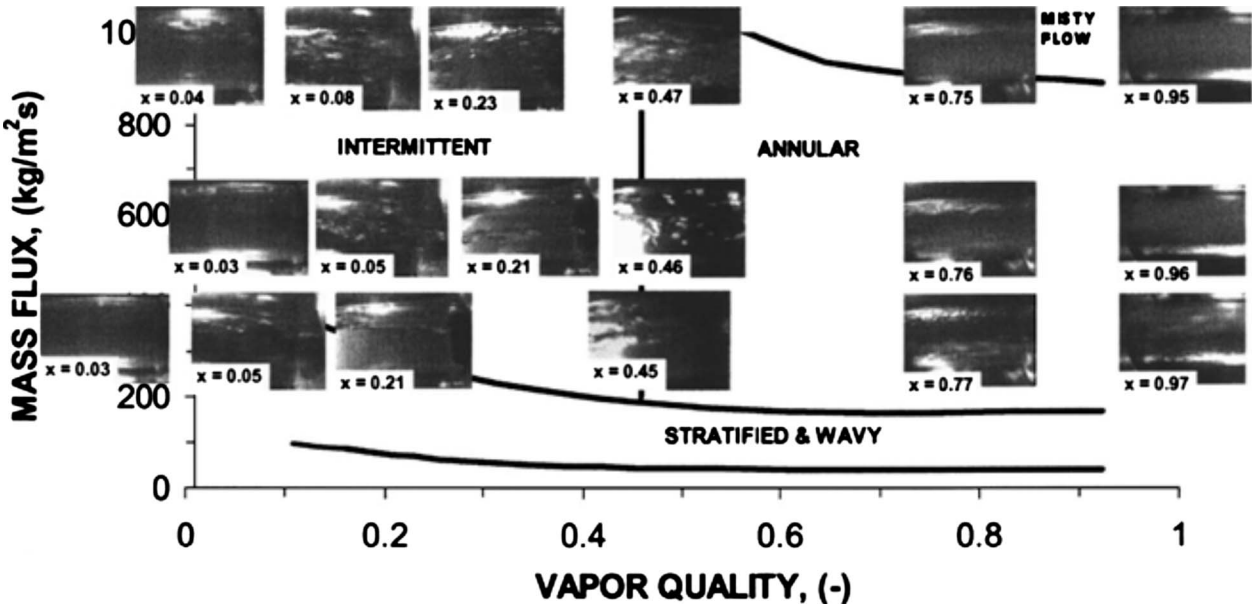

Fig. 21 Video images of condensing R-134a at 300 kg/m² s, 500 kg/m² s, and 800 kg/m² s in a smooth tube by Liebenberg and Meyer [136] superimposed on the map of El Hajal et al. [16]

Table 5 Summary of studies on flow patterns under microgravity conditions

Authors/References	Fluids and test section positions	Main research contents	Remarks
Zhao and Rezkallah [148]	Air-water, circular tube, 9.525 mm and 12.7 mm, vertical upward and down, bend and horizontal.	Flow patterns were studied and observed. Flow-pattern transition criteria were proposed.	Adiabatic cocurrent flow.
Rezkalleh [149]	Air-water, oil-water, R114 and water evaporation, horizontal and vertical.	Studies on flow patterns under microgravity conditions were summarized. The experimental data were compared to the available flow-pattern maps.	Adiabatic cocurrent flow.
Colin et al. [150]	Air-water, circular tube, 40 mm, horizontal.	Flow patterns were observed and flow transition was proposed.	Adiabatic cocurrent flow.
Dukler et al. [151]	Air-water, circular tube, 9.52 mm, horizontal.	Flow patterns and transitions were studied and flow maps were constructed.	Adiabatic cocurrent flow.
Rezkallah [152]	N/A	Weber number based flow-pattern maps were developed.	Adiabatic cocurrent flow.
Zhao and Wu [153]	N/A	A new model on slug to annular flow transition was proposed.	Adiabatic cocurrent flow
Bousman et al. [154]	Air-water, air-water/glycerin, air-water/zonyl, circular tubes, 12.7 mm and 25.4 mm, horizontal.	Flow patterns and transitions were studied and flow maps were constructed.	Adiabatic cocurrent flow.
Zhao et al. [155]	Carbogal-air, circular tube, 10 mm, horizontal.	Flow patterns were experimentally studied, and the experimental data were compared to the existing models.	Adiabatic cocurrent flow.
Celata et al. [156]	FC-72 evaporation, circular tubes, 4 mm and 6 mm, vertical.	Flow regimes were observed at normal and microgravity conditions. The flow-regime experimental data were compared to the available flow maps. A flow map was proposed.	Adiabatic cocurrent flow.

Table 6 Summary of studies on flow patterns in complex channels

Authors/References	Fluids and test section positions	Main research contents	Remarks
Murai et al. [163]	Air-water, helically coiled tube, vertical.	Flow patterns were experimentally studied and flow maps were constructed.	Adiabatic cocurrent flow.
Cotton et al. [164]	R134a evaporation, annular channels, horizontal.	Flow patterns under electrohydrodynamic (EHD) conditions were experimentally studied, and a flow-pattern map was constructed.	Adiabatic cocurrent flow.
Takeshima et al. [165,166]	Air-water, circular tube with a wire coil, vertical.	Flow patterns and transitions were studied and flow maps were constructed.	Adiabatic cocurrent flow.
Kim et al. [167]	Air-water, circular tube with a wire coil, vertical.	Flow patterns and transitions were studied and flow maps were constructed.	Adiabatic counter-current flow.
Wang et al. [168,169]	Air-water, circular return bends, horizontal.	The effect of return bends on flow patterns was studied and flow maps were constructed.	Adiabatic cocurrent flow.
Weisman et al. [170]	Air-water, R113 evaporation, circular tubes with helical wire ribs, horizontal.	The effect of fluid properties on flow patterns was studied.	Adiabatic cocurrent flow.
Weisman et al. [171]	Air-water, circular tubes with single and double helically ribs, horizontal.	Flow patterns were studied and compared to models.	Adiabatic cocurrent flow.
Hwang et al. [172]	Ethanol-CO_2, diverging and converging microchannels, horizontal.	Flow patterns were observed and analyzed.	Adiabatic cocurrent flow.

ticularly important since a unified model for predicting flow-pattern transitions for the whole range of pipe inclinations is presented. In addition, several studies have focused on specific flow-regime transitions such as the transition from stratified to slug and plug flow [186], the transition from stratified to slug regime in countercurrent flow [187], and the transition from bubble to slug flow [188] with a theoretical basis.

Modeling of Specific Flow Patterns. A number of studies have been conducted to model specific flow regimes such as stratified-wavy flow, intermittent flow, slug flow, and annular flow and to describe the flow regimes theoretically.

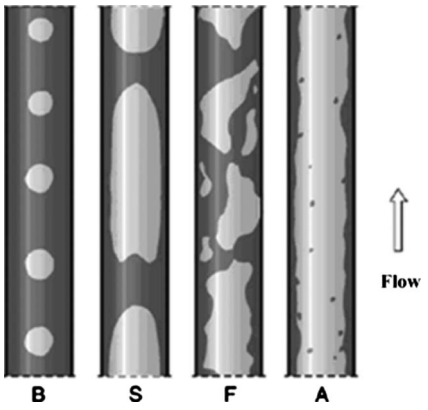

Fig. 22 Schematic flow patterns of highly viscous Newtonian fluid two-phase flow in vertical channels: *B*—bubble flow, *S*—slug flow, *F*—froth flow, and *A*—annular flow observed by Dziubinski et al. [175]

Liné and Lopez [189] developed a local two-fluid model for stratified flow. The key feature of their model lies in the transfer of momentum at the wavy gas-liquid surface that raises two important issues: the first is the deformation of the gas-liquid interface and the second is the distribution of the stresses over the wavy interface (pressure and viscous stresses). Brauner et al. [190] presented a straightforward extension of their two-fluid model for analyzing stratified flow with curved interfaces. The solution of the hydrodynamic model is combined with energy considerations to yield a complete solution for the interface configuration and the associated flow characteristics for a variety of two-fluid systems and under variable operational conditions. Agrawal et al. [191] presented an analysis of horizontal stratified two-phase flow in tubes. Nicholson et al. [192] developed predictive models for intermittent flow in horizontal tubes.

Taitel and Barnea [193] did a review of two-phase slug flow, which presents models of steady slug flow and transient slug flow for vertical, horizontal, and inclined channels. Fernandes et al. [194] developed a model for two-phase slug flow that can be used to predict many of the details of turbulent slug flow in vertical tubes, including average gas and liquid velocities in the slug and the Taylor bubbles separating successive slugs, the ratio of slug to bubble length, as well as the average voids in the slug. Moalem Maron et al. [195] studied the complexity of the hydrodynamic mechanisms in the mixing zone of slug flow by applying the k-l and k-ε models and numerically evaluated the various hydrodynamic characteristics. Particular boundary conditions at the free-moving interface were developed and incorporated in the numerical simulation. Taitel et al. [196] developed a slug flow model for downward inclined pipe flow, including a detailed description of the slug dissipation process in a downhill section and the calcula-

tion of slug dissipation distance. Barnea and Taitel [197] proposed a model for slug length distribution in gas-liquid slug flow, which assumes a random distribution at the inlet of the pipe and then calculates the increase or decrease in each individual slug length, including the disappearance of short slugs.

For evaporating two-phase flows in microchannels, Revellin et al. [90] and Agostini and Thome [214] proposed semitheoretical models to predict elongated bubble velocities and a new flow-pattern map based on the rate of bubble coalescence. Bubble frequencies first increased to a sharp peak and then rapidly decreased until annular flow was reached.

Analytical models of annular flow with and without entrainment have been derived from the mass, momentum and energy conservation equations with various assumptions [198,199]. Generally, some empirical correlations for the eddy diffusivity and liquid drop deposition rate are incorporated into the models. The book by Hewitt [198] presents details of annular flow models and is a good reference for this topic.

Studies on Flow Stability. Barnea and Taitel [200] studied structural and interfacial stability of multiple solutions for stratified flow. The solutions for stratified flow are considered using two types of stability analyses: structural stability analysis and interfacial stability analysis (Kelvin–Helmholtz stability). Brauner and Moalem Maron [201] proposed a new form for interfacial shear, which incorporates an explicit functional dependence on the interface slope due to interfacial waviness. It was shown that with the inclusion of the newly proposed dynamic term of interfacial shear, the stratified-smooth/stratified-wavy transitional boundary is satisfactorily predicted for a wide range of two-fluid systems. Barnea and Taitel [202] studied the neutral stability lines obtained from the viscous Kelvin–Helmholtz analysis and the inviscid analysis. It was shown that the stability behavior regarding the amplification rate is actually almost the same for the two analyses for a wide range of liquid viscosities and for various pipe inclinations. Barnea and Taitel [203] presented an overall review of the topic of stability of separated flows (stratified and annular flows). The stability of separated flows was examined using linear and nonlinear analyses. Both interfacial and structural stability analyses were made to obtain a complete view regarding the stability of the steady solutions and the resulting flow-pattern transition. Ying and Weisman [204] studied the relationship between interfacial shear and the flow patterns observed in the vertical upflow and downflow of vapor-liquid mixtures. The relationship between flow patterns and interfacial shear provides an alternative means of determining when flow transition occurs.

Besides the aforementioned theoretical studies in the literature, it should be mentioned that the intermolecular and surface forces are very important in understanding the theory of two-phase flows. On this aspect, the books by Ungarish [205] and by Israelachvili [206] are good references for a better understanding of gas-liquid two-phase flows from other viewpoints although they deal with hydrodynamics of suspensions, the forces between atoms and molecules, and the forces between particles and surfaces.

4 Applications

Flow patterns and flow-pattern maps are very important for the prediction of heat transfer coefficients and two-phase pressure drops. Even so, few such comprehensive models are available. They are briefly described in this section.

4.1 Flow-Pattern-Based Heat Transfer Prediction Methods. Heat transfer characteristics are intrinsically related to the corresponding flow patterns at diabatic conditions, such as for flow boiling or condensation, as shown in Figs. 3–5. Flow patterns can be used to explain physically the heat transfer trends, mechanisms, and phenomena. Vice versa, sharp changes in trends in local heat transfer coefficients can sometimes be used to back out the location of the corresponding flow-pattern transitions.

In the case of flow boiling, most of the leading heat transfer prediction methods are wholly empirical and do not include flow-pattern information [207,208]. The major deficiencies of these empirical correlations are as follows: (1) the predicted variations and peak in heat transfer coefficient versus vapor quality at a fixed mass velocity and heat flux often provide a poor match to those in the database; (2) the rapid falloff in heat transfer coefficient at high vapor quality is not predicted well; (3) the liquid convection coefficients are determined with turbulent flow correlations based on tubular flow rather than film flow (i.e., annular flow), and the two-phase convection multiplier should utilize the effective liquid velocity in the Reynolds number determined from the local void fraction to be consistent with the actual flow; (4) most correlations do not go to the natural limits of single-phase heat transfer at vapor quality $x=0$ (liquid flow) and $x=1$ (gas flow); (5) the effects of flow stratification on heat transfer have been developed primarily from a statistical analysis of the underlying heat transfer database using the liquid Froude number, a criterion that alone has been proven to be ineffective for predicting the onset of flow stratification (for horizontal and inclined tubes); (6) existing correlations have no mist flow nor partial dryout threshold criteria, erroneously using wet-wall correlations for evaporation for these conditions; (7) correlations ignore altogether the influence of two-phase flow structures. Therefore, there has been an attempt to develop flow-pattern-based heat transfer models to overcome these deficiencies over the past years.

Apparently, the first comprehensive flow-pattern-based flow boiling heat transfer model is that of Kattan et al. [10–12]. The model predicts local heat transfer coefficients based on the local flow patterns shown in Fig. 9 and has methods for predicting heat transfer coefficients in the annular, intermittent, stratified-wavy, and stratified flow regimes, where the choice of the method to use is determined locally with the associated flow-pattern map. The influences of void fraction and two-phase flow structure are introduced to obtain the annular film thickness, its film Reynolds number, and the fraction of the perimeter that is dry, if any. The Kattan–Thome–Favrat heat transfer model was developed for the evaporation of pure fluids (R134a and R123) and mixtures (azeotropic refrigerant mixture R502 and two near azeotropic mixtures R402A and R404A) inside plain horizontal macroscale tubes. However, their database did not include heat transfer coefficients for the stratified (S), bubbly (B), and mist flow (MF) regimes.

Modifications to the Kattan–Thome–Favrat flow-pattern map have been described in Sec. 2.2, and the heat transfer methods have been correspondingly modified. For example, Zürcher et al. [14] included a new onset of nucleate boiling criterion according to their flow boiling results for R134a, R407C, and R717 (ammonia). Wojtan et al. [18,19] extended the Kattan–Thome–Favrat [10–12] flow map to include a new dryout region and a new mist flow-regime transition and subdivided the stratified-wavy regime into three subregimes based on their observations and dynamic void fraction measurements for R22 and R410a. The new map is shown in Fig. 10, and they also developed the corresponding heat transfer methods for these regimes. Figure 10 also shows the predicted heat transfer coefficients (dashed line) for R22 at the indicated conditions. The flow-pattern-based heat transfer model predicted well their experimental data, as shown in Refs. [18,19].

Cheng et al. [20,21] recently developed a new heat transfer model for CO_2 evaporation using the model of Wojtan et al. [18,19] as their starting point. The method includes new correlations for the nucleate boiling heat transfer coefficients and a new boiling suppression factor based on the annular film thickness. In addition, new dryout inception and completion vapor quality correlations were proposed for CO_2, and a heat transfer correlation for the dryout region was obtained. Most of the heat transfer trends of CO_2 are captured by the new heat transfer model. Furthermore, new data allowed an updated model to be proposed for CO_2 [22,23]. The new flow map and flow-pattern-based heat transfer model cover the range of both macro- and microscale horizontal channels. A bubbly flow regime was added in the map

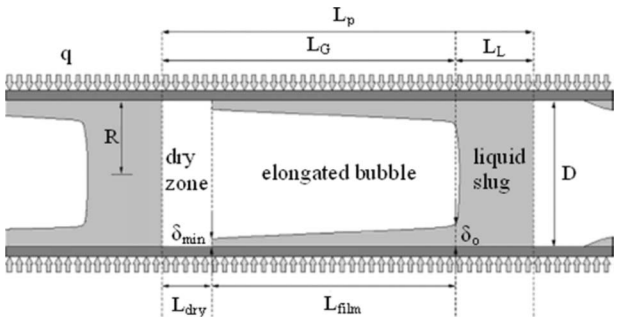

Fig. 23 Schematic of the three-zone evaporation model for elongated bubble flow regime by Thome et al. [212]

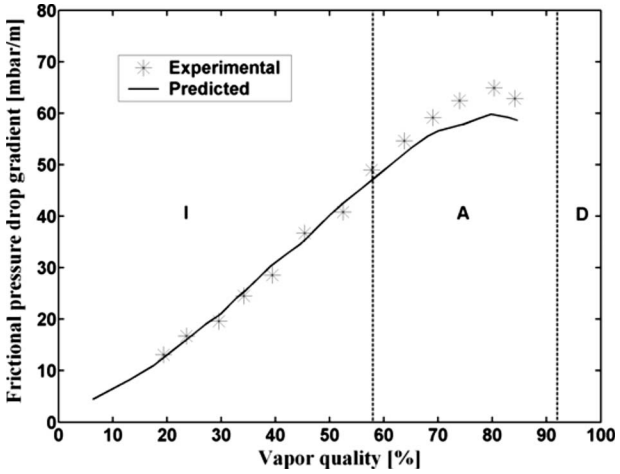

Fig. 24 Comparison of the predicted frictional pressure gradients by the Moreno-Quibén and Thome model to the experimental frictional pressure gradients for R410A at D=8 mm, T_{sat}=5°C, G=350 kg/m^2 s and q=6–9 kW/m^2, where 94.12% of the data were predicted within ±30% [34–36]

for the sake of completeness, and correspondingly a heat transfer model in the bubbly flow was suggested but still needs to be verified with experimental data. Furthermore, a heat transfer correlation in the mist flow regime was proposed based on the new flow map. Figure 11 shows the heat transfer coefficients (dashed line) for CO_2 predicted by the heat transfer model of Cheng et al. [22,23] evaluated for the indicated test conditions of Yun et al. [52] on the corresponding flow map. The heat transfer model predicted an extensive set of experimental data well and captured the sharp changes in trends in heat transfer, as shown in Ref. [23].

For convective condensation in horizontal plain macroscale tubes, El Hajal et al. [16] and Thome et al. [17] modified the Thome and El Hajal [15] flow map to apply it to condensing flows and proposed a flow-pattern-based heat transfer model somewhat similar to their flow boiling model, but including falling film condensation on "dry" perimeters and the effect of interfacial waves. Their model covered stratified, stratified-wavy, annular, and intermittent flows. Their flow-pattern-based condensation heat transfer model predicted their database well [16,17].

Kim and Ghajar [209] conducted an experimental study of heat transfer of air-water two-phase flow under uniform wall heat flux conditions without boiling and developed new two-phase heat transfer correlations that can be applied to air-water nonboiling two-phase heat transfer data in a horizontal pipe for different flow patterns. Recently, Kim and Ghajar [210] developed a general heat transfer coefficient correlation for horizontal gas-liquid flow for different flow patterns. In order to properly account for the effect of different flow patterns on the heat transfer in gas-liquid flow in a horizontal pipe, a flow-pattern factor was developed and introduced into their previous heat transfer correlation.

It should be mentioned that lubricant oil has a great effect on the heat transfer and pressure drops of refrigerants used in heat pumps, air conditioning, and refrigeration systems [207]. These include single-phase flow, flow boiling (evaporation), condensation, and supercritical processes such as the supercritical CO_2 cooling process [211]. In general, a small amount of oil tends to greatly decrease the heat transfer coefficients and increase the pressure drops. From the viewpoint of physical mechanisms, the flow patterns of oil-gas-liquid and oil-gas are very important in understanding the heat transfer and pressure drop characteristics, but little information on these flow patterns is available so far. Therefore, experiments are needed to investigate these flow patterns in both macro- and microchannels and to relate them to their corresponding heat transfer and pressure drop characteristics. Efforts should be made to develop flow-pattern-based heat transfer and pressure drop models in single-phase flow, flow boiling (evaporation), condensation, and supercritical processes based on a wide range of accurate experimental data and flow visualization.

In addition, heat transfer models for specific flow patterns have been studied. For instance, Taitel and Barnea [193] presented heat transfer models for slug flow. Cheng [199] studied models of annular flow heat transfer in a vertical smooth tube and a vertical spirally internally ribbed tubes. Thome et al. [212] and Dupont et al. [213] proposed a mechanistic heat transfer model to predict evaporation in the elongated bubble regime in microchannels with a three-zone flow boiling model describing the transient variation in the local heat transfer coefficient during sequential and cyclic passage of (i) a liquid slug, (ii) an evaporating elongated bubble, and (iii) a vapor slug when film dryout has occurred at the end of the elongated bubble. Figure 23 depicts a schematic of their model applicable to elongated bubble type flows. The model illustrates the strong dependency of heat transfer on fundamental characteristics of the two-phase flow, namely, the bubble frequency, the lengths of the bubbles and liquid slugs, and the initial liquid film thickness and its thickness at dryout. This model so far only covers heat transfer in the elongated bubble (slug) flow regime with and without intermittent dryout. Agostini and Thome [214] also made a preliminary extension to annular flows. For microscale channels, Thome [41] presented an overview of boiling and two-phase flows in microchannels and Ribatski et al. [215] presented a comprehensive analysis of the heat transfer prediction methods compared to an extensive database. As for the heat transfer prediction methods in microscale channels, efforts should be made to further achieve a complete flow-pattern-based heat transfer model.

4.2 Flow-Pattern-Based Pressure Drop Prediction Methods. The leading two-phase flow pressure drop prediction methods do not usually contain any flow-pattern information, and their use often causes errors of 50% or more for particular flow regimes [34–36,216,217]. The two-phase frictional pressure models available in the literature for horizontal flows have some or all of the following deficiencies: (1) they do not account for flow-pattern effects on the process, which are particularly important at low flow rates (stratification effects) and at high vapor qualities (for partial dryout and mist flows); (2) they do not account explicitly for the influence of interfacial waves; (3) they do not account for the upper dry perimeter of stratified types of flows; (4) they do not use the actual velocities of the vapor and liquid by the introduction of the local void fraction into the method; (5) they use tubular flow expressions to represent annular film flows; (6) they do not capture the peak in the pressure gradient at high vapor qualities (or its location or magnitude) nor give a good representation of the pressure gradient trend versus vapor quality; and (7) they do not go to acceptable limits at vapor quality, $x=0$ and $x=1$.

Flow patterns are intrinsically related to two-phase pressure drops due to the gas-liquid interfacial effect on the pressure drops. A phenomenological model relating the flow patterns to the cor-

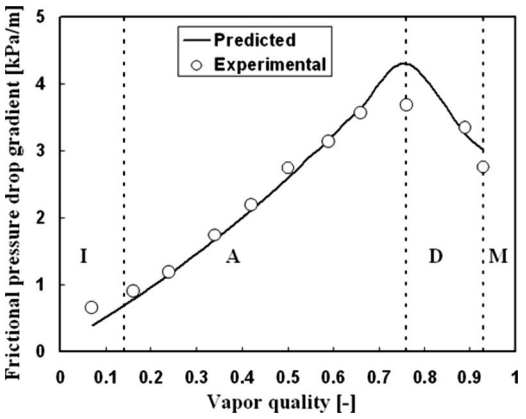

Fig. 25 Comparison of predicted frictional pressure gradient by the CO_2 pressure drop model of Cheng et al. [22] to the experimental data of Bredesen et al. [218] at the experimental conditions: G=400 kg/m^2 s, T_{sat}=−10°C, D=7 mm, and q =9 kW/m^2

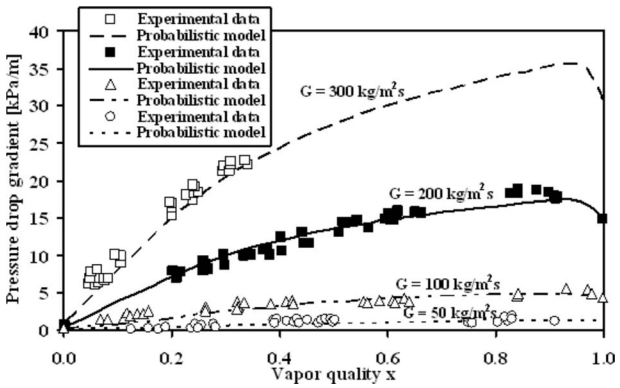

Fig. 26 Comparison of the predicted pressure drop gradients by the probabilistic model and the measured values for R134a at 10°C in six-port microchannels by Jassim and Newell [54]

responding pressure drops is a promising, more physically based approach. Hence, increasingly, attempts are being made to develop phenomenological models [217]. Moreno Quiben and Thome [34–36] recently proposed a new flow-pattern-based phenomenological model of two-phase frictional pressure drops. The new model was developed based on several simplified interfacial two-phase flow structures. The corresponding interfacial flow structures are determined using the flow-pattern map of Wojtan et al. [18,19]. Based on a statistical comparison, the new flow-pattern-based two-phase pressure drop model successfully predicted their experimental data and captured the trends and peaks observed in their data quite well. Figure 24 shows a comparison for the data in the intermittent, annular, and dryout (after the peak) regimes. Importantly, this completed an effort by Thome and coworkers to achieve a unified flow-pattern approach to model flow boiling, convective condensation, and two-phase pressure drops in horizontal tubes.

Based on the recent CO_2 flow-pattern map developed by Cheng et al. [22,23], a new two-phase frictional pressure drop model specifically for CO_2 was made by modifying the Moreno Quiben and Thome model [34–36] and incorporating the CO_2 flow-pattern map of Cheng et al. [22,23]. This is a phenomenological two-phase flow pressure drop model that is intrinsically related to the flow patterns. Figure 25 shows the comparison of the predicted and experimental pressure drop data of Bredesen et al. [218] in the intermittent, annular, dryout, and mist flows. The peak value predicted is the value at the transition between annular flow and mist flow. Good agreement has been obtained plus a good representation of the trends in the data. For the peak value, more experimental data in annular and mist flows are required to improve the model in the future. It should be mentioned that the two-phase pressure drop model developed by Cheng et al. [22] covers both macro- and microscale channels and thus also provides a prediction method for microscale channels. Further effort should be made to develop a generalized pressure drop model for microscale channels, which may be applied to a wide range of conditions and fluids.

Taking a different approach, Jassim and Newell [54] recently developed probabilistic methods to predict pressure drop and void fraction based on their probabilistic flow map shown in Fig. 12. Curve fits were made for flow-regime time fractions for R410A, R134a, and air-water at mass fluxes of 50 kg/m^2 s, 100 kg/m^2 s, 200 kg/m^2 s, and 300 kg/m^2 s for qualities from 0 to 1 by classifying observations into liquid, intermittent, vapor, and annular flow regimes. Pressure drop and void fraction correlations for each flow regime were chosen for incorporation into the microchannel models. The method is general, however, such that other correlations can be substituted if desired [54]. The total pressure drop is predicted as the sum of the flow-regime time fractions multiplied by the corresponding model for that flow regime. In this way, accurate models for the prediction of both pressure drop and void fraction in microchannels were developed, which incorporate flow-regime information in a full range of qualities and mass fluxes. Figure 26 shows the comparison of the predicted pressure drop gradients by the probabilistic model and the measured values for R134a at 10°C in six-port microchannels [54]. Further work is required to generalize their flow-regime time fraction correlations to additional test conditions.

5 Conclusions

This paper presents an overall survey and review of the studies on two-phase flow patterns and flow-pattern maps for a wide variety of flow channels and conditions. Through this comprehensive review, several research directions on the studies of flow patterns and flow-pattern maps have been identified and should be emphasized in the future as follows:

(1) In general, compared to that in macroscale channels, the study of flow patterns in microscale channels is still in its infancy. So far, although there are a number of studies on flow patterns and flow maps in microscale channels, there is no proven consistency of observations for the same fluids under the same test conditions taken by different researchers. Well documented theoretically based flow-pattern transition criteria and flow maps for microscale channels have not yet been established. Efforts should be made to achieve a systematic knowledge of these aspects.
(2) The studies of flow patterns and flow maps for tube bundles, during condensation, under microgravity conditions, and in complex channels are not sufficient for the development of general methods. Therefore, additional experimental efforts should be made to contribute to a systematic knowledge of these topics.
(3) Most researchers used traditional visual-only methods in their studies of flow regimes. These subjective methods generally lead to large errors in the flow-regime observations. This is the main reason why flow-pattern data from different researchers are often inconsistent for the same or similar test conditions. Contrary to the subjective methods, objective methods should be used to obtain more accurate flow-pattern data.
(4) Studies of the effects of channels shapes, physical properties, and adiabatic and diabatic conditions on flow regimes are still needed to complete our systematic knowledge of these topics. Especially, accurate diabatic flow-pattern data,

together with the corresponding heat transfer and pressure drop data, over a wide range of conditions are needed to develop or improve flow-pattern-based heat transfer and pressure drop prediction methods.

(5) Flow patterns of oil-gas-liquid and oil-gas are very important in understanding the lubricant oil effect of heat transfer and pressure drop characteristics in single-phase flow, flow boiling (evaporation), condensation, and supercritical processes, but little information on these flow patterns is available so far. Therefore, experiments are needed to investigate these flow patterns in both macro- and microchannels and to relate them to their corresponding heat transfer and pressure drop characteristics. Furthermore, flow-pattern-based heat transfer and pressure drop models should be developed based on a wide range of accurate experimental data and flow visualization.

References

[1] Collier, J. G., and Thome, J. R., 1994, *Convective Boiling and Condensation*, Oxford University Press, New York.

[2] Carey, V. P., 1992, *Liquid Vapor Phase Change Phenomena*, Hemisphere, Washington D.C.

[3] Hewitt, G. F., 1982, "Liquid-Gas Systems," in *Handbook of Multiphase Systems*, G. Hetsroni, ed., Hemisphere, Washington, D.C.

[4] Thome, J. R., 2006, *Wolverine Engineering Databook III*, available for free at the following website: http://www.wlv.com/products/databook/db3/DataBookIII.pdf

[5] Hewitt, G. F., and Roberts, D. N., 1969, "Studies of Two-Phase Flow Patterns by Simultaneous X-Ray and Flash Photography," Atomic Energy Research Establishment, Harwell, Report No. AERE-M 2159.

[6] Baker, O., 1954, "Simultaneous Flow of Oil and Gas," Oil Gas J., **53**, pp. 185–190.

[7] Taitel, Y., and Dukler, A. E., 1976, "A Model for Predicting Flow Regime Transitions in Horizontal and Near Horizontal Gas-Liquid Flow," AIChE J., **22**, pp. 47–55.

[8] Hashizume, K., 1983, "Flow Pattern and Void Fraction of Refrigerant Two-Phase Flow in a Horizontal Pipe," Bull. JSME, **26**, pp. 1597–1602.

[9] Steiner, D., 1993, *VDI-Wärmeatlas*, Verein Deutscher Ingenieure VDI-Gessellschaft Verfahrenstechnik und Chemieingenieurwessen (GCV), Düsseldorf, Chap. Hbb.

[10] Kattan, N., Thome, J. R., and Favrat, D., 1998, "Flow Boiling in Horizontal Tubes—Part I: Development of a Diabatic Two-Phase Flow Pattern Map," ASME J. Heat Transfer, **120**, pp. 140–147.

[11] Kattan, N., Thome, J. R., and Favrat, D., 1998, "Flow Boiling in Horizontal Tubes—Part II: New Heat Transfer Data for Five Refrigerants," ASME J. Heat Transfer, **120**, pp. 148–155.

[12] Kattan, N., Thome, J. R., and Favrat, D., 1998, "Flow Boiling in Horizontal Tubes—Part III: Development of a New Heat Transfer Model Based on Flow Patterns," ASME J. Heat Transfer, **120**, pp. 156–165.

[13] Zürcher, O., Thome, J. R., and Favrat, D., 1999, "Evaporation of Ammonia in a Smooth Horizontal Tube: Heat Transfer Measurements and Predictions," ASME J. Heat Transfer, **121**, pp. 89–101.

[14] Zürcher, O., Favrat, D., and Thome, J. R., 2002, "Development of Diabatic Two-Phase Flow Pattern Map for Horizontal Flow Boiling," Int. J. Heat Mass Transfer, **45**, pp. 291–301.

[15] Thome, J. R., and El Hajal, J., 2002, "Two-Phase Flow Pattern Map for Evaporation in Horizontal Tubes: Latest Version," *1st International Conference on Heat Transfer, Fluid Mechanics and Thermodynamics*, Kruger Park, South Africa, pp. 182–188.

[16] El Hajal, J., Thome, J. R., and Cavallini, A., 2003, "Condensation in Horizontal Tubes, Part 1: Two-Phase Flow Pattern Map," Int. J. Heat Mass Transfer, **46**, pp. 3349–3363.

[17] Thome, J. R., El Hajal, J., and Cavallini, A., 2003, "Condensation in Horizontal Tubes, Part 2: New Heat Transfer Model Based on Flow Regimes," Int. J. Heat Mass Transfer, **46**, pp. 3365–3387.

[18] Wojtan, L., Ursenbacher, T., and Thome, J. R., 2005, "Investigation of Flow Boiling in Horizontal Tubes, Part 1: A New Diabatic Two-Phase Flow Pattern Map," Int. J. Heat Mass Transfer, **48**, pp. 2955–2969.

[19] Wojtan, L., Ursenbacher, T., and Thome, J. R., 2005, "Investigation of Flow Boiling in Horizontal Tubes, Part 2—Development of a New Heat Transfer Model for Stratified-Wavy, Dryout and Mist Flow Regimes," Int. J. Heat Mass Transfer, **48**, pp. 2970–2985.

[20] Cheng, L., Ribatski, G., Wojtan, L., and Thome, J. R., 2006, "New Flow Boiling Heat Transfer Model and Flow Pattern Map for Carbon Dioxide Evaporating Inside Horizontal Tubes," Int. J. Heat Mass Transfer, **49**, pp. 4082–4094.

[21] Cheng, L., Ribatski, G., Wojtan, L., and Thome, J. R., 2007, "Erratum to: New Flow Boiling Heat Transfer Model and Flow Pattern Map for Carbon Dioxide Evaporating Inside Tubes [Heat Mass Transfer 49(21–22) (2006) 4082–4094]," Int. J. Heat Mass Transfer, **50**, p. 391.

[22] Cheng, L., Ribatski, G., Quibén Moreno, T., and Thome, J. R., 2008, "New Prediction Methods for CO_2 Evaporation inside Tubes, Part 1—A Two-Phase Flow Pattern Map and a Flow Pattern Based Phenomenological Model for Two-Phase Flow Frictional Pressure Drops," Int. J. Heat Mass Transfer, **51**, pp. 111–124.

[23] Cheng, L., Ribatski, G., and Thome, J. R., 2008, "New Prediction Methods for CO_2 Evaporation Inside Tubes, Part 2—An Updated General Flow Boiling Heat Transfer Model Based on Flow Patterns," Int. J. Heat Mass Transfer, **51**, pp. 125–135.

[24] Martinelli, R. C., and Nelson, D. B., 1948, "Prediction of Pressure Drop During Forced Circulation Boiling of Water," Trans. ASME, **70**, pp. 695–702.

[25] Lockhart, R. W., and Martinelli, R. C., 1949, "Proposed Correlation of Data for Isothermal Two-Phase Two-Component Flow in a Pipe," Chem. Eng. Prog., **45**, pp. 39–48.

[26] Chisholm, D., 1973, "Pressure Gradients Due to Friction During the Flow of Evaporating Two-Phase Mixtures in Smooth Tubes and Channels," Int. J. Heat Mass Transfer, **16**, pp. 347–358.

[27] Grönnerud, R., 1979, "Investigation of Liquid Hold-Up, Flow-Resistance and Heat Transfer in Circulation Type of Evaporators, Part IV: Two-Phase Flow Resistance in Boiling Refrigerants," in *Annexe 1972.1, Bull. De l'Inst. Du Froid*.

[28] Müller-Steinhagen, H., and Heck, K., 1986, "A Simple Friction Pressure Correlation for Two-Phase Flow in Pipes," Chem. Eng. Process., **20**, pp. 297–308.

[29] Friedel, L., 1979, "Improved Friction Pressure Drop Correlations for Horizontal and Vertical Two-Phase Pipe Flow," *European Two-Phase Flow Group Meeting*, Ispra, Italy, Paper No. E2.

[30] Chen, J. C., 1966, "Correlation for Boiling Heat Transfer to Saturated Fluids in Convective Flow," I&EC Process Des. Dev., **5**, pp. 322–339.

[31] Shah, M. M., 1982, "Chart Correlation for Saturated Boiling Heat Transfer: Equations and Further Study," ASHRAE Trans., **88**, pp. 185–196.

[32] Gungor, K. E., and Winterton, R. H. S., 1986, "A General Correlation for Flow Boiling in Tubes and Annuli," Int. J. Heat Mass Transfer, **29**, pp. 351–358.

[33] Kandlikar, S. G., 1990, "A General Correlation for Saturated Two-Phase Flow Boiling Heat Transfer Inside Horizontal and Vertical Tubes," ASME J. Heat Transfer, **112**, pp. 219–228.

[34] Moreno Quibén, J., and Thome, J. R., 2007, "Flow Pattern Based Two-Phase Frictional Pressure Drop Model for Horizontal Tubes, Part I: Diabatic and Adiabatic Experimental Study," Int. J. Heat Fluid Flow, **28**, pp. 1049–1059.

[35] Moreno Quibén, J., and Thome, J. R., 2007, "Flow Pattern Based Two-Phase Frictional Pressure Drop Model for Horizontal Tubes, Part II: New Phenomenological Model," Int. J. Heat Fluid Flow, **28**, pp. 1060–1072.

[36] Moreno Quibén, J., 2005, *Experimental and Analytical Study of Two-Phase Pressure Drops During Evaporation in Horizontal Tubes*, Ph.D. thesis, Swiss Federal Institute of Technology (EPFL), Lausanne, Switzerland.

[37] Rouhani, S. Z., and Sohal, M. S., 1983, "Two-Phase Flow Patterns: A Review of Research Results," Prog. Nucl. Energy, **11**(3), pp. 219–259.

[38] Kandlikar, S. G., 2002, "Fundamental Issues Related to Flow Boiling in Minichannels and Microchannels," Exp. Therm. Fluid Sci., **26**, pp. 389–407.

[39] Cheng, L., Mewes, D., and Luke, A., 2007, "Boiling Phenomena With Surfactants and Polymeric Additives: A State-of-the-Art Review," Int. J. Heat Mass Transfer, **50**, pp. 2744–2771.

[40] Thome, J. R., 2004, "Boiling in Microchannels: A Review of Experiment and Theory," Int. J. Heat Fluid Flow, **25**, pp. 128–139.

[41] Thome, J. R., 2006, "State-of-the Art Overview of Boiling and Two-Phase Flows in Microchannels," Heat Transfer Eng., **27**(9), pp. 4–19.

[42] Cheng, L., and Mewes, D., 2006, "Review of Two-Phase Flow and Flow Boiling of Mixtures in Small and Mini Channels," Int. J. Multiphase Flow, **32**, pp. 183–207.

[43] Kew, P. A., and Cornwell, K., 1997, "Correlations for the Prediction of Boiling Heat Transfer in Small-Diameter Channels," Appl. Therm. Eng., **17**, pp. 705–715.

[44] Thome, J. R., and Ribatski, G., 2006, "State-of-the Art of Two-Phase Flow and Flow Boiling and Pressure Drop of CO_2 in Macro- and Micro-Channels," Int. J. Refrig., **28**, pp. 1149–1168.

[45] Shah, R. K., 1986, "Classification of Heat Exchangers," *Heat Exchangers: Thermal Hydraulic Fundamentals and Design*, S. Kakac, A. E. Bergles, and F. Mayinger, eds., Hemisphere, Washington, D.C., pp. 9–46.

[46] Mehendale, S. S., Jacobi, A. M., and Ahah, R. K., 2000, "Fluid Flow and Heat Transfer at Micro- and Meso-Scales With Application to Heat Exchanger Design," Appl. Mech. Rev., **53**, pp. 175–193.

[47] Triplett, K. A., Ghiaasiaan, S. M., Abdel-Khalik, S. I., and Sadowski, D. L., 1999, "Gas-Liquid Two-Phase Flow in Microchannels. Part I: Two-Phase Flow Patterns," Int. J. Multiphase Flow, **25**, pp. 377–394.

[48] Brauner, N., and Moalem-Maron, D., 1992, "Identification of the Range of Small Diameter Conduits Regarding Two-Phase Flow Pattern Transitions," Int. Commun. Heat Mass Transfer, **19**, pp. 29–39.

[49] Palen, J. W., Breber, G., and Taborek, K., 1979, "Prediction of Flow Regimes in Horizontal Tube-Side-Condensation," Heat Transfer Eng., **1**(2), pp. 47–57.

[50] Troniewski, L., and Ulbrich, R., 1984, "The Analysis of Flow Regime Maps of Two-Phase Gas-Liquid Flow in Pipes," Chem. Eng. Sci., **39**, pp. 1213–1224.

[51] Chisholm, D., 1983, *Two-Phase Flow in Pipelines and Heat Exchangers*, Longman, New York.

[52] Yun, R., Kim, Y., and Kim, M. S., 2005, "Flow Boiling Heat Transfer of Carbon Dioxide in Horizontal Mini Tubes," Int. J. Heat Fluid Flow, **26**, pp. 801–809.

[53] Niño, V. G., 2002, "Characterization of Two-Phase Flow in Microchannels," Ph.D. thesis, University of Illinois, Urbana-Champaign, IL.

[54] Jassim, E. W., and Newell, T. A., 2006, "Prediction of Two-Phase Pressure

Drop and Void Fraction in Microchannels Using Probabilistic Flow Regime Mapping," Int. J. Heat Mass Transfer, **49**, pp. 2446–2457.
[55] Jassim, E. W., 2006, "Probabilistic Flow Regime Map Modeling of Two-Phase Flow," Ph.D. thesis, University of Illinois, Urbana-Champaign, IL.
[56] Jassim, E. W., Newell, T. A., and Chato, J. C., 2007, "Probabilistic Determination of Two-Phase Flow Regimes in Horizontal Tubes Utilizing an Automated Image Recognition Techniques," Exp. Fluids, **42**, pp. 563–573.
[57] Ebner, L., Drahos, J., Ebner, G., and Cermak, J., 1987, "Characterization of Hydrodynamics Regimes in Horizontal Two-Phase Flow Part I: Pressure Drop Measurements," Chem. Eng. Process., **22**, pp. 39–43.
[58] Drahos, J., Cermak, J., Selucky, K., and Ebner, L., 1987, "Characterization of Hydrodynamics Regimes in Horizontal Two-Phase Flow Part II: Analysis of Wall Pressure Fluctuations," Chem. Eng. Process., **22**, pp. 45–52.
[59] Pazsit, I., 1986, "Two-Phase Flow Identification by Correlation Techniques," Ann. Nucl. Energy, **13**(1), pp. 37–41.
[60] Barnea, D., Shoham, O., and Taitel, Y., 1980, "Flow Pattern Characterization in Two-Phase Flow by Electrical Conductance Probe," Int. J. Multiphase Flow, **6**, pp. 387–397.
[61] Matsui, G., 1984, "Identification of Flow Regimes in Vertical Gas-Liquid Two-Phase Flow Using Differential Pressure Fluctuations," Int. J. Multiphase Flow, **6**, pp. 711–720.
[62] Hervieu, E., Seleghim, P., Jr., 1998, "An Objective Indicator for Two-Phase Flow Pattern Transition," Nucl. Eng. Des., **184**, pp. 421–435.
[63] Hsieh, C. C., Wang, S. B., and Pan, C., 1997, "Dynamic Visualization of Two-Phase Flow Patterns in a Natural Circulation Loop," Int. J. Multiphase Flow, **23**, pp. 1147–1170.
[64] Geiger, A. B., Tsukada, A., Lehmann, E., Vontobel, P., Wokaun, A., and Scherer, G. G., 2002, "In Situ Investigation of Two-Phase Flow Patterns in Flow Fields of PEFC's Using Neutron Radiography," Fuel Cells, **2**, pp. 92–98.
[65] Tutu, N. K., 1982, "Pressure Fluctuations and Flow Pattern Recognition in Vertical Two Phase Gas-Liquid Flows," Int. J. Multiphase Flow, **8**, pp. 443–447.
[66] Thomson, O., and Pazsit, I., 1995, "The Crossed Beam Correlation Technique for Two-Phase Flow Measurements," Prog. Nucl. Energy, **29**, pp. 337–346.
[67] Weisman, J., and Kang, S. Y., 1981, "Flow Pattern Transitions in Vertical and Upwardly Inclined Lines," Int. J. Multiphase Flow, **7**, pp. 271–291.
[68] Stanislav, J. F., Kokal, S., and Nicholson, M. K., 1986, "Intermittent Gas-Liquid Flow in Upward Inclined Pipes," Int. J. Multiphase Flow, **12**, pp. 325–335.
[69] Rozenblit, R., Gurevich, M., Lengel, Y., and Hetsroni, G., 2006, "Flow Patterns and Heat Transfer in Vertical Upward Air-Water Flow With Surfactant," Int. J. Multiphase Flow, **32**, pp. 889–901.
[70] Furukawa, T., and Fukano, T., 2001, "Effect of Liquid Viscosity on Flow Patterns in Vertical Upward Gas-Liquid Two-Phase Flow," Int. J. Multiphase Flow, **27**, pp. 1109–1126.
[71] Zapke, A., and Kröger, D. G., 2000, "Countercurrent Gas-Liquid Flow in Inclined and Vertical Ducts—I: Flow Patterns, Pressure Drop Characteristics and Flooding," Int. J. Multiphase Flow, **26**, pp. 1439–1455.
[72] Hasan, A. R., and Kabir, C. S., 1992, "Two-Phase Flow in Vertical and Inclined Annuli," Int. J. Multiphase Flow, **18**, pp. 279–293.
[73] Govier, G. W., and Short Leigh, W., 1958, "The Upward Vertical Flow of Air-Water Mixtures," Can. J. Chem. Eng., **36**, pp. 195–202.
[74] Crawford, T. J., Weinberger, C. B., and Weisman, J., 1985, "Two-Phase Flow Patterns and Void Fractions in Downward Flow. Part I: Steady-State Flow Patterns," Int. J. Multiphase Flow, **11**, pp. 761–782.
[75] Crawford, T. J., Weinberger, C. B., and Weisman, J., 1986, "Two-Phase Flow Patterns and Void Fractions in Downward Flow. Part II: Void Fractions and Transient Flow Patterns," Int. J. Multiphase Flow, **12**, pp. 219–236.
[76] Weisman, J., Duncan, D., Gibson, J., and Grawford, T., 1979, "Effect of Fluid Properties and Pipe Diameter on Two-Phase Flow Patterns in Horizontal Lines," Int. J. Multiphase Flow, **5**, pp. 437–462.
[77] Govier, G. W., and Omer, M. M., 1962, "The Pipeline Flow of Air-Water Mixtures," Can. J. Chem. Eng., **51**, pp. 93–104.
[78] Hand, N. P., and Spedding, P. L., 1993, "Horizontal Gas-Liquid Flow at Close to Atmospheric Conditions," Chem. Eng. Sci., **48**, pp. 2283–2305.
[79] Lin, P. Y., and Hanratty, T. J., 1987, "Effect of Pipe Diameter on Flow Patterns for Air-Water Flow in Horizontal Pipes," Int. J. Multiphase Flow, **13**, pp. 549–563.
[80] Mukherjee, H., and Brill, J. P., 1985, "Empirical Equations to Predict Flow Patterns in Two-Phase Inclined Flow," Int. J. Multiphase Flow, **11**, pp. 299–315.
[81] Hashizume, K., 1983, "Flow Pattern, Void Fraction and Pressure Drop of Refrigerant Two-Phase Flow in a Horizontal Pipe I. Experimental Data," Int. J. Multiphase Flow, **9**, pp. 399–410.
[82] Filippov, Yu. P., 1999, "Characteristics of Horizontal Two-Phase Helium Flows Part I: Flow Patterns and Void Fraction," Cryogenics, **39**, pp. 59–68.
[83] Alexeyev, A. I., Filippov, Yu. P., and Madedov, I. S., 1991, "Flow Patterns of Two-Phase Helium in Horizontal Channels," Cryogenics, **31**, pp. 330–337.
[84] Barnea, D., Shoham, O., and Taitel, Y., 1980, "Flow Pattern Transition for Gas-Liquid Flow in Horizontal and Inclined Pipes," Int. J. Multiphase Flow, **6**, pp. 217–225.
[85] Wolk, G., Dreyer, M., and Rath, H. J., 2000, "Flow Patterns in Small Diameter Vertical Non-Circular Channels," Int. J. Multiphase Flow, **26**, pp. 1037–1061.
[86] Ghajar, A. J., 2004, "Two-Phase Heat Transfer in Gas-Liquid Non-Boiling Pipe Flows," *Proceedings of the 3rd International Conference on Heat Transfer, Fluid Mechanics and Thermodynamics (HEFAT 2004)*, Cape Town, South Africa.
[87] Woldesemayat, M. A., and Ghajar, A. J., 2007, "Comparison of Void Fraction Correlations for Different Flow Patterns in Horizontal and Upward Inclined Pipes," Int. J. Multiphase Flow, **33**, pp. 347–370.
[88] Ghiaasiaan, S. M., and Abdel-Khalik, S. I., 2001, "Two-Phase Flow in Microchannels," Adv. Heat Transfer, **34**, pp. 145–254.
[89] Suo, M., and Griffith, P., 1964, "Two-Phase Flow in Capillary Tubes," ASME J. Basic Eng., **86**, pp. 576–582.
[90] Revellin, R., Dupont, V., Ursenbacher, T., Thome, J. R., and Zun, I., 2006, "Characterization of Diabatic Two-Phase Flows in Microchannels: Flow Parameter Results for R-134a in a 0.5 mm Channel," Int. J. Multiphase Flow, **32**, pp. 755–774.
[91] Revellin, R., and Thome, J. R., 2006, "Experimental Two-Phase Fluid Flow in Microchannels," *4th Japanese-European Two-Phase Flow Group Meeting*, Kanbaikan, Kyoto, Sept. 24–28.
[92] Revellin, R., and Thome, J. R., 2007, "Experimental Investigation of R-134a and R-245fa Two-Phase Flow in Microchannels for Different Flow Conditions," Int. J. Heat Fluid Flow, **28**, pp. 63–71.
[93] Revellin, R., and Thome, J. R., 2007, "New Type of Diabatic Flow Pattern Map for Boiling Heat Transfer in Microchannels," J. Micromech. Microeng., **17**, pp. 788–796.
[94] Cubaud, T., and Ho, C.-M., 2004, "Transport of Bubbles in Square Microchannels," Phys. Fluids, **16**, pp. 4575–4585.
[95] Coleman, J. W., and Garimella, S., 1999, "Characterization of Two-Phase Flow Patterns in Small Diameter Round and Rectangular Tubes," Int. J. Heat Mass Transfer, **42**, pp. 2869–2881.
[96] Chen, T., and Garimella, S. V., 2006, "Measurements and High-Speed Visualizations of Flow Boiling of a Dielectric Fluids in a Silicon Microchannel Heat Sink," Int. J. Multiphase Flow, **32**, pp. 957–971.
[97] Zhao, T. S., and Bi, Q. C., 2001, "Co-Current Air-Water Two-Phase Flow Patterns in Vertical Triangular Microchannels," Int. J. Multiphase Flow, **27**, pp. 765–782.
[98] Yun, R., and Kim, Y., 2004, "Flow Regimes for Horizontal Two-Phase Flow of CO_2 in a Heated Narrow Rectangular Channel," Int. J. Multiphase Flow, **30**, pp. 1259–1270.
[99] Pettersen, J., 2004, "Flow Vaporization of CO_2 in Microchannel Tubes," Exp. Therm. Fluid Sci., **28**, pp. 111–121.
[100] Lowry, B., and Kawaji, M., 1988, "Adiabatic Vertical Two-Phase Flow in Narrow Flow Channels," Int. J. Heat Exchangers, **84**(263), pp. 133–139.
[101] Damianides, C. A., and Westwater, J. W., 1988, "Two-Phase Flow Patterns in a Compact Heat Exchanger and in Small Tubes," *Proceedings of the 2nd U.K. National Conference on Heat Transfer*, Vol. 2, pp. 1257–1268.
[102] Yang, C. Y., and Shieh, C. C., 2001, "Flow Pattern of Air-Water and Two-Phase R-134a in Small Circular Tubes," Ind. Eng. Chem. Res., **27**, pp. 1163–1177.
[103] Huh, C., and Kim, M. H., 2006, "An Experimental Investigation of Flow Boiling in an Asymmetrically Heated Rectangular Microchannel," Exp. Therm. Fluid Sci., **30**, pp. 775–784.
[104] Hardt, S., Schilder, B., Tiemann, D., Kolb, G., Hessel, V., and Stephan, P., 2007, "Analysis of Flow Patterns Emerging During Evaporation in Parallel Microchannels," Int. J. Heat Mass Transfer, **50**, pp. 226–239.
[105] Owhaib, W., Palm, B., and Martin-Callizo, C., 2006, "Flow Boiling Visualization in a Vertical Circular Minichannel at High Vapor Quality," Exp. Therm. Fluid Sci., **30**, pp. 755–763.
[106] Sobierska, E., Kulenovic, R., Mertz, R., and Groll, M., 2007, "Experimental Results of Flow Boiling of Water in a Vertical Microchannels," Exp. Therm. Fluid Sci., **31**, pp. 111–119.
[107] Yen, T. H., Shoji, M., Takemura, F., Suzuki, Y., and Kasage, N., 2006, "Visualization of Convective Boiling Heat Transfer in Single Microchannels With Different Shaped Cross-Sections," Int. J. Heat Mass Transfer, **49**, pp. 3884–3894.
[108] Ekberg, N. P., Ghiaasiaan, S. M., Abdel-Khalik, S. I., Yoda, M., and Jeter, S. M., 1999, "Gas-Liquid Two-Phase Flow in Narrow Horizontal Annuli," Nucl. Eng. Des., **192**, pp. 59–80.
[109] Fukano, T., Kariyasaki, A., and Kagawa, M., 1989, "Flow Patterns and Pressure Drop in Isothermal Gas-Liquid Concurrent Flow in a Horizontal Capillary Tube," *ANS Proceedings of the National Heat Transfer Conference*, IL, Vol. 4, pp. 153–161.
[110] Serizawa, A., Feng, Z., and Kawara, Z., 2002, "Two-Phase Flow in Microchannels," Exp. Therm. Fluid Sci., **26**, pp. 703–714.
[111] Ide, H., Kariyasaki, A., and Fukano, T., 2007, "Fundamental Data on the Gas-Liquid Two-Phase Flow in Microchannels," Int. J. Therm. Sci. **46**, pp. 519–530.
[112] Satitchaicharoen, P., and Wongwises, S., 2004, "Two-Phase Flow Pattern Maps for Vertical Upward Gas-Liquid Flow in Mini-Gap Channels," Int. J. Multiphase Flow, **30**, pp. 225–236.
[113] Li, J., and Peterson, G. P., 2005, "Boiling Nucleation and Two-Phase Flow Patterns in Forced Liquid Flow in Microchannels," Int. J. Heat Mass Transfer, **48**, pp. 4797–4810.
[114] Barajas, A. M., and Panton, R. L., 1993, "The Effects of Contact Angle on Two-Phase Flow in Capillary Tubes," Int. J. Multiphase Flow, **19**, pp. 337–346.
[115] Hetsroni, G., Mosyak, A., Segal, Z., and Pogrebnyak, E., 2003, "Two-Phase Flow Patterns in Parallel Micro-Channels," Int. J. Multiphase Flow, **29**, pp. 341–360.
[116] Kawahara, A., Chung, P. M.-Y., and Kawaji, M., 2002, "Investigation of

Two-Phase Flow Pattern, Void Fraction and Pressure Drop in Microchannel," Int. J. Multiphase Flow, **28**, pp. 1411–1435.
[117] Chung, P. M.-Y., and Kawaji, M., 2004, "The Effect of Channel Diameter on Adiabatic Two-Phase Flow Characteristics in Microchannels," Int. J. Multiphase Flow, **30**, pp. 735–761.
[118] Nakoryakov, V. E., Kuznetsov, V. V., and Vitovsky, O. V., 1992, "Experimental Investigation of Upward Gas-Liquid Flow in a Vertical Narrow Annulus," Int. J. Multiphase Flow, **18**, pp. 313–326.
[119] Fukano, T., and Kariyasaki, A., 1993, "Characteristics of Gas-Liquid Two-Phase Flow in a Capillary Tube," Nucl. Eng. Des., **141**, pp. 59–68.
[120] Wambsganss, M. W., Jendrzejczyk, J. A., and France, D. M., 1991, "Two-Phase Flow Patterns and Transitions in a Small, Horizontal, Rectangular Channel," Int. J. Multiphase Flow, **17**, pp. 327–342.
[121] Tabatabai, A., and Faghri, A., 2001, "A New Two-Phase Flow Map and Transition Boundary Accounting for Surface Tension Effects in Horizontal Miniature and Micro Tubes," ASME J. Heat Transfer, **123**, pp. 958–968.
[122] Ullmann, A., and Brauner, N., 2006, "The Prediction of Flow Pattern Maps in Mini Channels," *4th Japanese-European Two-Phase Flow Group Meeting*, Kanbaikan, Kyoto, Sept. 24–28.
[123] Ullmann, A., and Brauner, N., 2007, "The Prediction of Flow Pattern Maps in Microchannels," Multiphase Sci. Technol., **19**(1), pp. 49–73.
[124] Revellin, R., and Thome, J. R., 2008, "A Theoretical Model for the Prediction of the Critical Heat Flux in Heated Microchannels," Int. J. Heat Mass Transfer, **51**, pp. 1216–1225.
[125] Ribatski, G., and Thome, J. R., 2007, "Two-Phase Flow and Heat Transfer Across Horizontal Bundles—A Review," Heat Transfer Eng., **28**(6), pp. 508–524.
[126] Ribatski, G., and Thome, J. R., 2004, "Dynamics of Two-Phase Flow Across Horizontal Tube Bundles—A Review," *Proceedings of the 10th Brazilian Congress of Thermal Sciences and Engineering—ENCIT 2004*, Rio de Janeiro, Brazil, Nov. 20–Dec. 3.
[127] Casciaro, S., and Thome, J. R., 2001, "Thermal Performance of Flooded Evaporators, Part 1: Review of Boiling Heat Transfer Studies," ASHRAE Trans., **107**, pp. 903–918.
[128] Casciaro, S., and Thome, J. R., 2001, "Thermal Performance of Flooded Evaporators, Part 2: Review of Void Fraction, Two-Phase Pressure Drop, and Flow Pattern Studies," ASHRAE Trans., **107**, pp. 919–930.
[129] Venkateswararao, P., Semiat, R., and Dukler, A. E., 1982, "Flow Pattern Transition for Gas-Liquid Flow in a Vertical Rod Bundle," Int. J. Multiphase Flow, **8**, pp. 509–524.
[130] Aprin, L., Mercier, P., and Tadrist, L., 2007, "Experimental Analysis of Local Void Fractions Measurements for Boiling Hydrocarbons in Complex Geometry," Int. J. Multiphase Flow, **33**, pp. 371–393.
[131] Narrow, T. L., Ghiaasiaan, S. M., Abdel-Khalik, S. I., and Sadowski, D. L., 2000, "Gas-Liquid Two-Phase Flow Patterns and Pressure Drop in a Horizontal Micro-Rod Bundle," Int. J. Multiphase Flow, **26**, pp. 1281–1294.
[132] Ulbrich, R., and Mewes, D., 1994, "Vertical, Upward Gas-Liquid Two-Phase Flow Across a Tube Bundle," Int. J. Multiphase Flow, **20**, pp. 249–272.
[133] Noghrehkar, G. R., Kawaji, M., and Chan, A. M. V., 1999, "Investigation of Two-Phase Flow Regimes in Tube Bundles Under Cross-Flow Condition," Int. J. Multiphase Flow, **25**, pp. 857–874.
[134] Xu, G. P., Tso, C. P., and Tou, K. W., 1998, "Hydrodynamics of Two-Phase Flow in Vertical Up- and Down-Flow Across a Horizontal Tube Bundle," Int. J. Multiphase Flow, **24**, pp. 1317–1342.
[135] Grant, I. D. R., and Chisholm, D., 1979, "Two-Phase Flow on the Shell-Side of a Segmentally Baffled Shell and Tube Heat Exchanger," ASME J. Heat Transfer, **101**, pp. 38–42.
[136] Liebenberg, L., Thome, J. R., and Meyer, J. P., 2005, "Flow Visualization and Flow Pattern Identification With Power Spectral Density Distributions of Pressure Traces During Refrigerant Condensation in Smooth and Micro-Fin Tubes," ASME J. Heat Transfer, **127**, pp. 209–220.
[137] Liebenberg, L., and Meyer, J. P., 2006, "The Characterization of Flow Regimes With Power Spectral Density Distributions of Pressure Fluctuations During Condensation in Smooth and Micro-Fin Tubes," Exp. Therm. Fluid Sci., **31**, pp. 127–140.
[138] Olivier, J. A., Liebenberg, L., Thome, J. R., and Meyer, J. P., 2007, "Heat Transfer, Pressure Drop, and Flow Pattern Recognition During Condensation inside Smooth, Helical Micro-Fin, and Herringbone Tubes," Int. J. Refrig., **30**, pp. 609–623.
[139] Louahlia-Gualous, H., and Mecheri, B., 2007, "Unsteady Steam Condensation Flow Patterns Inside a Miniature Tube," Appl. Therm. Eng., **27**, pp. 1225–1235.
[140] Mederic, B., Miscevic, M., Platel, V., Lavieille, P., and Joly, J.-L., 2004, "Experimental Study of Flow Characteristics During Condensation in Narrow Channels: The Influence of the Diameter Channel on Structure Patterns," Superlattices Microstruct., **35**, pp. 573–586.
[141] Mederic, B., Lavieille, P., and Miscevic, M., 2006, "Heat Transfer Analysis According to Condensation Flow Structures in a Minichannel," Exp. Therm. Fluid Sci., **30**, pp. 785–793.
[142] Chen, Q., Amano, R. S., and Xin, M., 2006, "Experimental Study of Flow Patterns and Regimes of Condensation in Horizontal Three-Dimensional Micro-Fin-Tubes," IEEE Commun. Mag., **43**, pp. 201–206.
[143] Chen, Y., and Cheng, P., 2005, "Condensation of Steam in Silicon Microchannels," Int. Commun. Heat Mass Transfer, **32**, pp. 175–183.
[144] Coleman, J. W., and Garimella, S., 2003, "Two-Phase Flow Regimes in Round, Square and Rectangular Tubes During Condensation of Refrigerant R134a," Int. J. Refrig., **26**, pp. 117–128.
[145] Cheng, L., and Yang, J., 1998, "A New Treated Surface for Achieving Dropwise Condensation," J. Enhanced Heat Transfer, **5**(1), pp. 1–8.
[146] Cheng, L., and van der Geld, C. W. M., 2005, "Experimental Study of Heat Transfer and Pressure Drop Characteristics of Air/Water and Air-Steam/Water Heat Exchange in a Polymer Compact Heat Exchanger," Heat Transfer Eng., **26**(2), pp. 18–27.
[147] Cheng, L., van der Geld, C. W. M., and Lexmond, A. S., 2004, "Study and Visualization of Droplet Entrainment From a Polymer Compact Heat Exchanger," Int. J. Heat Exchangers, **5**, pp. 359–378.
[148] Zhao, L., and Rezkallah, K. S., 1993, "Gas-Liquid Flow Patterns at Microgravity Conditions," Int. J. Multiphase Flow, **19**, pp. 751–763.
[149] Rezkallah, K. S., 1990, "A Comparison of Existing Flow-Pattern Predictions During Forced-Convective Two-Phase Flow Under Microgravity Conditions," Int. J. Multiphase Flow, **16**, pp. 243–259.
[150] Colin, C., Fabre, J., and Dukler, A. E., 1991, "Gas-Liquid Flow at Microgravity Conditions—I: Dispersed Bubble and Slug Flow," Int. J. Multiphase Flow, **17**, pp. 533–544.
[151] Dukler, A. E., Fabre, J. A., McQuillen, J. B., and Vernon, R., 1988, "Gas-Liquid Flow at Microgravity Conditions: Flow Patterns and Their Transitions," Int. J. Multiphase Flow, **14**, pp. 389–400.
[152] Rezkallah, K. S., 1996, "Weber Number Based Flow Pattern Maps for Liquid-Gas Flows at Microgravity," Int. J. Multiphase Flow, **22**, pp. 1265–1270.
[153] Zhao, J. F., and Wu, W. R., 2000, "Slug to Annular Flow Transition of Microgravity Two-Phase Flow," Int. J. Multiphase Flow, **26**, pp. 1295–1304.
[154] Bousman, W. S., McQuillen, J. B., and Witte, L. C., 1996, "Gas-Liquid Flow Patterns in Microgravity: Effects of Tube Diameter, Liquid Viscosity and Surface Tension," Int. J. Multiphase Flow, **22**, pp. 1035–1053.
[155] Zhao, J. F., Xie, J. C., Lin, H., Hu, W. R., Ivanov, A. V., and Belyaev, A. Yu., 2001, "Experimental Studies on Two-Phase Flow Patterns Aboard the Mir Space Station," Int. J. Multiphase Flow, **27**, pp. 1931–1944.
[156] Celata, G. P., Cumo, M., Gervasi, M., and Zummo, G., 2006, "Flow Pattern Analysis of Flow Boiling in Microgravity," *4th Japanese-European Two-Phase Flow Group Meeting*, Kanbaikan, Kyoto, Sept. 24–28.
[157] Ohta, H., 2003, "Microgravity Heat Transfer in Flow Boiling," Adv. Heat Transfer, **37**, pp. 1–76.
[158] Cheng, L., and Chen, T., 2006, "Enhanced Heat Transfer Characteristics of Upward Flow Boiling of Kerosene in a Vertical Spirally Internally Ribbed Tube," Chem. Eng. Technol., **29**, pp. 1233–1241.
[159] Cheng, L., and Chen, T., 2001, "Flow Boiling Heat Transfer in a Vertical Spirally Internally Ribbed Tube," Heat Mass Transfer, **37**, pp. 229–236.
[160] Cheng, L., and Xia, G., 2002, "Experimental Study of CHF in a Vertical Spirally Internally Ribbed Tube Under the Condition of High Pressures," Int. J. Therm. Sci., **41**, pp. 396–400.
[161] Cheng, L., and Chen, T., 2001, "Study of Flow Boiling Heat Transfer in a Tube With Axial Microgrooves," Exp. Heat Transfer, **14**(1), pp. 59–73.
[162] Thome, J. R., 1990, *Enhanced Boiling Heat Transfer*, Hemisphere, New York.
[163] Murai, Y., Yoshikawa, S., Toda, S. I., Ishikawa, M. A., and Yamamoto, F., 2006, "Structure of Air-Water Two-Phase Flow in Helically Coiled Tubes," Nucl. Eng. Des., **236**, pp. 94–106.
[164] Cotton, J., Robinson, A. J., Shoukri, M., and Chang, J. S., 2005, "A Two-Phase Flow Pattern Map for Annular Channels Under a DC Applied Voltage and the Application to Electrohydrodynamic Convective Boiling Analysis," Int. J. Heat Mass Transfer, **48**, pp. 5563–5579.
[165] Takeshima, K., Fujii, T., Takenaka, N., and Asano, H., 2002, "The Flow Characteristics of an Upward Gas-Liquid Two-Phase Flow in a Vertical Tube With a Wire Coil: Part 1. Experimental Results of Flow Pattern, Void Fraction, and Pressure Drop," Heat Transfer Asian Res., **31**(8), pp. 639–651.
[166] Takeshima, K., Fujii, T., Takenaka, N., and Asano, H., 2002, "The Flow Characteristics of an Upward Gas-Liquid Two-Phase Flow in a Vertical Tube With a Wire Coil: Part 2. Effect on Void Fraction and Liquid Film Thickness," Heat Transfer Asian Res., **31**(8), pp. 652–664.
[167] Kim, H. Y., Koyama, S., and Matsumoto, W., 2001, "Flow Pattern and Flow Characteristics for Counter-Current Two-Phase Flow in a Vertical Round Tube With Wire-Coil Inserts," Int. J. Multiphase Flow, **27**, pp. 2063–2081.
[168] Wang, C. C., Chen, I. Y., Yang, Y. W., and Hu, R., 2004, "Influence of Horizontal Return Bend on the Two-Phase Flow Pattern in Small Diameter Tubes," Exp. Therm. Fluid Sci., **28**, pp. 145–152.
[169] Wang, C. C., Chen, I. Y., Yang, Y. W., and Chang, Y. J., 2003, "Two-Phase Flow Pattern in Small Diameter Tubes With the Presence of Horizontal Return Bend," Int. J. Heat Mass Transfer, **46**, pp. 2975–2981.
[170] Weisman, J., Lan, J., and Disimile, P., 1996, "The Effect of Fluid Properties on Two-Phase (Vapor-Liquid) Flow Patterns in the Presence of Helical Wire Ribs," Int. J. Multiphase Flow, **22**, pp. 613–619.
[171] Weisman, J., Lan, J., and Disimile, P., 1994, Two-Phase (Air-Water) Flow Patterns and the Pressure Drop in the Presence of Helical Wire Ribs, Int. J. Multiphase Flow, **20**, pp. 885–889.
[172] Hwang, J. J., Tseng, F. G., and Pan, C., 2005, "Ethanol-CO_2 Two-Phase Flow in Diverging and Converging Microchannels," Int. J. Multiphase Flow, **31**, pp. 548–570.
[173] Shirai, H., Sadatomi, M., and Kawahara, A., 2006, "Gas-Liquid Con-Current and Counter-Current Diversion Cross-Flow Between Subchannels in Vertical 2×1 Rod Channel," *4th Japanese-European Two-Phase Flow Group Meeting*, Kanbaikan, Kyoto, Sept. 24–28.
[174] Chhabra, R. P., and Richardson, J. F., 1984, "Prediction of Flow Patterns for Cocurrent Flow of Gas and Non-Newtonian Liquid in Horizontal Pipes,"

Can. J. Chem. Eng., **62**, pp. 449–454.
[175] Dziubinski, M., Fidos, H., and Sosno, M., 2004, "The Flow Pattern Map of a Liquid-Gas Flow in the Vertical Pipe," Int. J. Multiphase Flow, **30**, pp. 551–563.
[176] Taitel, Y., Lee, N., and Dukler, A. E., 1978, "Transient Gas-Liquid Flow in Horizontal Pipes: Modeling the Flow Pattern Transitions," AIChE J., **24**, pp. 920–934.
[177] Taitel, Y., Barnea, D., and Dukler, A. E., 1980, "Modeling Flow Pattern Transitions for Steady Upward Gas-Liquid Flow in Vertical Tubes," AIChE J., **26**, pp. 345–354.
[178] Taitel, Y., and Barnea, D., 1983, "Counter Current Gas-Liquid Vertical Flow, Model for Flow Pattern and Pressure Drop," Int. J. Multiphase Flow, **9**, pp. 637–647.
[179] Ito, K., Inoue, M., Ozawa, M., and Shoji, M., 2004, "A Simplified Model of Gas-Liquid Two-Phase Flow Pattern Transition," Heat Transfer Asian Res., **33**(7), pp. 445–461.
[180] Crawford, T., and Weisman, J., 1984, "Two-Phase (Vapor-Liquid) Flow Pattern Transitions in Ducts of Non-Circular Cross-Section and Under Diabatic Conditions," Int. J. Multiphase Flow, **10** pp. 385–391.
[181] McQuillan, K., and Whalley, P. B., 1985, "Flow Patterns in Vertical Two-Phase Flow," Int. J. Multiphase Flow, **11**, pp. 161–175.
[182] Bilicki, Z., and Kestin, J., 1987, "Transition Criteria for Two-Phase Flow Patterns in Vertical Upward Flow," Int. J. Multiphase Flow, **13**, pp. 283–294.
[183] Mishima, K., and Ishii, M., 1984, "Flow Regime Transition Criteria for Upward Two-Phase Flow in Vertical Tubes," Int. J. Heat Mass Transfer, **27**, pp. 723–737.
[184] Hibiki, T., and Mishima, K., 2001, "Flow Regime Transition Criteria for Upward Two-Phase Flow in Vertical Narrow Rectangular Channels," Nucl. Eng. Des., **203**, pp. 117–131.
[185] Barnea, D., 1987, "A Unified Model for Predicting Flow-Pattern Transitions for the Whole Range of Pipe Inclinations," Int. J. Multiphase Flow, **13**, pp 1–12.
[186] Hurlburt, E. T., and Hanratty, T. J., 2002, "Prediction of the Transition From Stratified to Slug and Plug Flow for Long Pipes," Int. J. Multiphase Flow, **28**, pp. 707–729.
[187] Johnston, A. J., 1985, "Transition From Stratified to Slug Regime in Countercurrent Flow," Int. J. Multiphase Flow, **11**, pp. 31–41.
[188] Matuszkiewicz, A., Flamand, J. C., and Boure, J. A., 1987, "The Bubble-Slug Flow Pattern Transition and Instabilities of Void Fraction Waves," Int. J. Multiphase Flow, **13**, pp. 199–217.
[189] Liné, A., and Lopez, D., 1997, "Two-Fluid Model of Wavy Separated Two-Phase Flow," Int. J. Multiphase Flow, **23**, pp. 1131–1146.
[190] Brauner, N., Moalem Maron, D., and Rovinsky, J., 1998, "A Two-Fluid Model for Stratified Flows With Curved Interfaces," Int. J. Multiphase Flow, **24**, pp. 975–1004.
[191] Agrawal, S. S., Gregory, G. A., and Govier, G. W., 1973, "An Analysis of Horizontal Stratified Two Phase Flow on Pipes," Can. J. Chem. Eng., **51**, pp. 280–286.
[192] Nicholson, M. K., Aziz, K., and Gregory, G. A., 1978, "Intermittent Two Phase Flow in Horizontal Pipes: Predictive Models," Can. J. Chem. Eng., **56**, pp. 653–663.
[193] Taitel, Y., and Barnea, D., 1990, "Two-Phase Slug Flow," Adv. Heat Transfer, **20**, pp. 83–132.
[194] Fernandes, R. C., Semiat, R., and Dukler, A. E., 1983, "Hydrodynamic Model for Gas-Liquid Slug Flow in Vertical Tubes," AIChE J., **29**, pp. 981–989.
[195] Moalem Maron, D., Yacoub, N., Brauner, N., and Daot, D., 1991, "Hydrodynamic Mechanisms in the Horizontal Slug Pattern," Int. J. Multiphase Flow, **17**, pp. 227–245.
[196] Taitel, Y., Sarica, C., and Brill, J. P., 2000, "Slug Flow Modeling for Downward Inclined Pipe Flow: Theoretical Considerations," Int. J. Multiphase Flow, **26**, pp. 833–844.
[197] Barnea, D., and Taitel, Y., 1993, "A Model for Slug Length Distribution in Gas-Liquid Slug Flow," Int. J. Multiphase Flow, **19**, pp. 829–838.
[198] Hewitt, G. F., 1970, *Annular Two-Phase Flow*, Pergamon, Oxford.
[199] Cheng, L., 2007, "Modelling of Heat Transfer of Upward Annular Flow in Vertical Tubes," Chem. Eng. Commun., **194**, pp. 975–993.
[200] Barnea, D., and Taitel, Y., 1992, "Structural and Interfacial Stability of Multiple Solutions for Stratified Flow," Int. J. Multiphase Flow, **18**, pp. 821–830.
[201] Brauner, N., and Moalem Maron, D., 1993, "The Role of Interfacial Shear Modeling in Predicting the Stability of Stratified Two-Phase Flow," Chem. Eng. Sci., **48**, pp. 2867–2879.
[202] Barnea, D., and Taitel, Y., 1993, "Kelvin-Helmholtz Stability Criteria for Stratified Flow: Viscous Versus Non-Viscous (Inviscid) Approaches," Int. J. Multiphase Flow, **19**, pp. 639–649.
[203] Barnea, D., and Taitel, Y., 1994, "Interfacial and Structural Stability of Separated Flow," Int. J. Multiphase Flow, **20**, pp. 387–414.
[204] Ying, A., and Weisman, J., 1989, "The Relationship Between Interfacial Shear and Flow Pattern in Vertical Flow," Int. J. Multiphase Flow, **15**, pp. 23–34.
[205] Ungarish, M., 1993, *Hydrodynamics of Suspensions*, Springer-Verlag, Berlin.
[206] Israelachvili, S., 1997, *Intermolecular and Surface Forces*, Academic, San Diego.
[207] Thome, J. R., Cheng, L., Ribatski, G., and Vales, L. F., 2008, "Flow Boiling of Ammonia and Hydrocarbons: A State-of-the-Art Review," Int. J. Refrig., **31**, pp. 603–620.
[208] Cheng, L., and Chen, T., 2000, "Comparison of Six Typical Correlations for Upward Flow Boiling Heat Transfer With Kerosene in a Vertical Smooth Tube," Heat Transfer Eng., **21**(5), pp. 27–34.
[209] Kim, D., and Ghajar, A. J., 2002, "Heat Transfer Measurements and Correlations for Air-Water Flow of Different Flow Patterns in a Horizontal Pipe," Exp. Therm. Fluid Sci., **25**, pp. 659–676.
[210] Kim, J.-Y., and Ghajar, A. J., 2006, "A General Heat Transfer Correlation for Non-Boiling Gas-Liquid Flow With Different Flow Patterns in Horizontal Pipes," Int. J. Multiphase Flow, **32**, pp. 447–465.
[211] Cheng, L., Ribatski, G., and Thome, J. R., 2008, "Analysis of Supercritical CO_2 Cooling in Macro- and Micro Channels," Int. J. Refrig., doi: 10.1016/j.ijrefrig.2008.010.
[212] Thome, J. R., Dupont, V., Jacobi, and A. M., 2004, "Heat Transfer Model for Evaporation in Microchannels. Part I: Presentation of the Model," Int. J. Heat Mass Transfer, **47**, pp. 3375–3385.
[213] Dupont, V., Thome, J. R., and Jacobi, A. M., 2004, "Heat Transfer Model for Evaporation in Microchannels. Part II: Comparison With the Database," Int. J. Heat Mass Transfer, **47**, pp. 3387–3401.
[214] Agostini, B., and Thome, J. R., 2005, "Comparison of an Extended Database for Flow Boiling Heat Transfer Coefficients in Multi-Microchannels Elements With the Three-Zone Model," *ECI Heat Transfer and Fluid Flow in Microscale*, Casrelvecchio Pascoli, Italy.
[215] Ribatski, G., Wojtan, L., and Thome, J. R., 2006, "An Analysis of Experimental Data and Prediction Methods for Two-Phase Frictional Pressure Drop and Flow Boiling Heat Transfer in Micro-Scale Channels," Exp. Therm. Fluid Sci., **31**, pp. 1–19.
[216] Cheng, L., and Chen, T., 2007, "Study of Vapor Liquid Two-Phase Frictional Pressure Drop in a Vertical Heated Spirally Internally Ribbed Tube," Chem. Eng. Sci., **62**, pp. 783–792.
[217] Ould-Didi, M. B., Kattan, N., and Thome, J. R., 2002, "Prediction of Two-Phase Pressure Gradients of Refrigerants in Horizontal Tubes," Int. J. Refrig., **25**, pp. 935–947.
[218] Bredesen, A., Hafner, A., Pettersen, J., Neksa, P., and Aflekt, K., 1997, "Heat Transfer and Pressure Drop for In-Tube Evaporation of CO_2," *Intenational Conference on Heat Transfer Issues in Natural Refrigerants*, University of Maryland.

Lixin Cheng *is a scientific collaborator at the Laboratory of Heat and Mass Transfer at the Swiss Federal Institute of Technology in Lausanne (EPFL), Switzerland since 2006. He received his Ph.D. at the State Key Laboratory of Multiphase Flow at Xi'an Jiaotong University, China in 1998. He was awarded an Alexander von Humboldt Fellowship and thus worked in the Institute of Process Engineering at the Leibniz University of Hanover, Germany from 2004 to 2006. He was a senior research fellow at the London South Bank University from 2001 to 2003 and a postdoctoral research fellow at the Eindhoven University of Technology, The Netherlands from 2000 to 2001. His research interests include multiphase flow and heat transfer, enhanced heat transfer, microscale heat transfer, nanofluid two-phase flow and heat transfer, compact and microheat exchangers, and thermal systems. He has published more than 60 papers in journals and conferences. He is a member of the Editorial Advisory Board of The Open Thermodynamics Journal and is a reviewer for 15 international journals.*

Gherhardt Ribatski *is a collaborating professor of the Department of Mechanical Engineering at the University of São Paulo (USP) in São Carlos, Brazil since August 2006. He received his BS in 1995, MS in 1998, and Ph.D. in 2002, all in Mechanical Engineering from the University of São Paulo, Brazil. He was a postdoctoral researcher in the Department of Mechanical and Industrial Engineering at University of Illinois at Urbana-Champaign from 2002 to 2003 and a postdoctoral researcher in the Laboratory of Heat and Mass Transfer at the Swiss Federal Institute of Technology in Lausanne (EPFL), Switzerland from 2003 to 2006. His research interests cover pool boiling, falling-film evaporation and condensation, two-phase flow, boiling and condensation of external and internal flow, and convective evaporation and condensation in microscale channels. He has published more than 40 papers on these subjects.*

John R. Thome *is professor and director at the Laboratory of Heat and Mass Transfer at the Swiss Federal Institute of Technology in Lausanne (EPFL), Switzerland since 1998, where his primary interests of research are two-phase flow and heat transfer, covering both macro- and microscale heat transfer and also enhanced heat transfer. He received his Ph.D. at Oxford University, England in 1978 and was formerly a professor at Michigan State University. From 1984 to 1998, he managed his own international engineering consulting company. He is the author of three books: Enhanced Boiling Heat Transfer (1990), Convective Boiling and Condensation, 3rd edition (1994), and Wolverine Engineering Databook III (2004), and has another new book coming out entitled Nucleate Boiling on Microstructured Surfaces (2008). He received the ASME Heat Transfer Division's Best Paper Award in 1998 for a three-part paper on flow boiling heat transfer published in the Journal of Heat Transfer. He has published more than 100 journal papers since joining the EPFL and is also active in giving international short courses on selected topics in two-phase flow and heat transfer.*